Semi-Annual Report on

Coupling Processes

between

Atmospheric Chemistry and Climate

NAS5-97039

by

M. K. W. Ko, Debra Weisenstein, Run-Lie Shia, and N. D. Sze

Atmospheric and Environmental Research, Inc.

840 Memorial Drive

Cambridge, MA 02139

Prepared for

NASA Atmospheric Chemistry Modeling and Data Analysis Program

March 1, 1998

Table of Content

Abstract

This is the second semi-annual report for NAS5-97039. Work in this project is related to NAS1-20666, also funded by NASA ACMAP. The overall objective of this project is to improve the understanding of coupling processes between atmospheric chemistry and climate. Model predictions of the future distributions of trace gases in the atmosphere constitute an important component of the input necessary for quantitative assessments of global change. We will concentrate on the changes in ozone and stratospheric sulfate aerosol, with emphasis on how ozone in the lower stratosphere would respond to natural or anthropogenic changes.

The key modeling tools for this work are the AER two-dimensional chemistry-transport model, the AER two-dimensional stratospheric sulfate model, and the AER three-wave interactive model with full chemistry. We will continue developing our three-wave model so that we can help NASA determine the strength and weakness of the next generation assessment models.

(I) Two-dimensional Chemistry-Transport Model

(I.1) Model Enhancements

The following model enhancements were implemented in the past 6 months, primarily for the purpose of performing the WMO/UNEP ozone trends calculations. (1) We downloaded from the Goddard DAAC reanalyzed temperature data from NCEP for the 1987-1995 period. This complements the 1979-1986 data we had obtained in 1996. The data was processed into monthly average zonal means and monthly temperature probability statistics on the AER 2-D CTM grid. We have used the data both to generate climatological temperature and temperature distributions for the entire 1979-1995 period, and for calculation of historical ozone trends employing the actual temperature for each year between 1979 and 1995. (2) The reaction $ClO+OH \rightarrow HCl+O_2$ was added to the 2-D CTM. Though it has been know for some time that use of this reaction would improve agreement between models and measurements near 40 km, a definitive measurement of the rate constant was not made until 1997 when Lipson et al. (1997) measured the branching ratio for the ClO+OD reaction and found 5-6% branching to DCl. (3) Five additional CFC and HCFC species were added to the model in order to account for future CFC substitutes in our ozone trends calculation. These were CFC-114, CFC-115, HCFC-141b, HCFC-142b, and HCFC-123.

(I.2) Studies and Publications related to the 2-D CTM

(I.2.1) ODP of CH_3Br

We submitted a paper to the *Journal of Geophysical Research* on the ozone depletion potential (ODP) of CH_3Br. The ODP of CH_3Br is determined by combining the model calculated ODP/BLP ratio (where BLP is the bromine loading potential) for CH_3Br and its atmospheric lifetime. This paper examines how changes in several key kinetic data affect the ODP/BLP ratio. The key reactions highlighted in this study include the reaction of $BrO+HO_2$, the absorption cross-section of HOBr, the absorption cross-section and the photolysis products of $BrONO_2$, and the heterogeneous conversion of $BrONO_2$ to HOBr and HNO_3 on aerosol particles. By combining the calculated ODP/BLP ratio with the latest estimate of 0.7 year for the atmospheric lifetime of CH_3Br, the likely value of ODP for CH_3Br is 0.39. The model calculated concentration of HBr (~ 0.3 pptv) in the lower stratosphere is substantially smaller than the reported measured value of about 1.5 pptv. The model can reproduce the measured value of 1.5 pptv if one assumes a yield for HBr of

1.3% from the reaction of BrO+OH, or a yield of 0.6% from the reaction of BrO + HO_2. Our calculations show that the effect of these assumed rates on the model calculated ODP/BLP ratio is minimal: practically no impact for the assumed BrO+OH yield and 10% smaller for the BrO+HO_2 case.

A copy of the manuscript is included as an appendix.

(I.2.2). Adjusting K_{yy} in 2-D CTM according to observations

a) Using exchanging rates to adjust K_{yy} in subtropics

The subtropical barrier reduces the mixing between the tropics and the mid-latitudes in the lower stratosphere, and has significant effects on tracer distribution in the stratosphere. It is important for 2-D CTMs to have a realistic exchange rate between the tropics and mid-latitudes to simulate the effects of the subtropical barrier. The exchange rate is determined by the eddy diffusion coefficient K_{yy} in the model. In an earlier study, we introduced a tropical pipe by reducing the K_{yy} in the tropics from 0.3 to 0.03 (10^6 m^2/sec), (Weisenstein, et al. 1996). Recently, *in situ* measurements of chemical species with a wide range of local lifetimes have been used to quantify the air exchange rate between the tropics and mid-latitudes in the lower stratosphere from the tropopause to around 21 km. It is found that the mid-latitude air is entrained into the tropical lower stratosphere with a replacement time scale of 10-18 months (Minschwaner et al., 1996; Volk et al., 1996). Meanwhile, Schoeberl et al. (1997) estimate the mixing time between the tropics and mid-latitudes in the 20-28 km region to be at least 18 months using the QBO signals in N_2O/CH_4 ratio and tropical winds from UARS measurements. These results demonstrate that the tropical barrier allows a moderate penetration.

The horizontal diffusion fluxes and the mixing ratio of CCl_4, CF_2Cl_2, $CFCl_3$, CH_3CCl_3, CH_4, HNO_3, N_2O, NO_y, and O_3 calculated in the AER 2-D model are used to derive the exchange rates between the tropical and the mid-latitudes in the lower stratosphere. They are compared with the exchange rates estimated from observations. Using the original model (global diffuser model) with a K_{yy} of 0.3 x 10^6 m^2/sec in the lower tropical stratosphere the model calculated exchange time scales are around 5-6 months. The tropical pipe model results show a much slower exchange rate of 38-60 months. Our studies showed that values for K_{yy} of 0.13 x 10^6 m^2/sec from the tropopause

to 21 km and 0.07 x 10^6 m^2/sec from 21 km to 35 km in the model (leaky pipe model) will generate an exchange time scale of around 14 months below 20 km and 18 months in the 20-30 km region, in good agreement with the estimates from observations.

The model calculated lifetimes for species like N_2O and CFCs in the leaky pipe model are reduced by about 10% compared to the global diffuser model. Our model results show that the calculated ozone response to HSCT engine emissions is also smaller in the leaky pipe model.

The paper that summarizes the results of this study was sent to *Journal of Geophysical Research* for publication. Two reviewers have made some suggestions and we are in the process of revision. The revised version was sent back to *Journal of Geophysical Research* in February 1998.

b) Using latitudinal gradient of N_2O and NO_y/O_3 to adjust K_{yy} near polar vortex

It is well know that the isolation of the polar vortex is one of the preconditions for the Antarctic ozone hole to be developed (WMO 1988). The mixing ratio of long-lived tracers like CH4 and N2O usually are quite different inside and outside of the vortex due to the isolation of the vortex and the descending motion of the air inside the vortex during the polar winter night. The potential vorticity (PV), which is a good dynamic tracer, has been used to define the boundary of the vortex where the PV has large horizontal gradients (Manning et al., 1995). The gradient of the long-lived tracers across the vortex is usually underestimated in 2-D model simulations. There are two dynamical parameters in AER 2-D CTM which affect the horizontal gradient of long-lived species around the vortex, K_{yy} and the circulation. We found that the value of K_{yy} currently used in AER 2-D CTM during the winter high latitudes is probably too large to maintain sharp gradients for long-lived species near the polar vortex. We put a polar barrier in the model by reducing Kyy from 10^{10} cm^2/sec to 10^8 cm^2/sec between 50° to 70° during the winter. It is found that the horizontal gradient of N_2O and the ratio of NO_y/O_3 near the vortex is quite sensitive to the change of K_{yy}. Fig. 1 shows the model calculated annually averaged ratio of NO_y/O_3 at 64 mb with and without the polar barrier along with the observations. The polar barrier seems to have improved the model simulation. The generalized coordinate method, reported at the M&MII workshop (1997) by David Considine of GFSC, used to process UARS N_2O data

produces larger gradient of N_2O near the polar vortex than ordinary zonally average does. We will use this method to process UARS N_2O, NO_y and O_3 data and use their gradient near the polar vortex to fine-tune K_{yy} in the polar region.

(II) 2-D Interactive Model

(II. 1) Improvements of the 3-wave Model

The current version of the AER 3-wave interactive model has a vertical resolution of 3.5 km. In order to meet the future requirement for assessment studies, the resolution should be increased especially near the tropopause so that the exchange between the troposphere and the stratosphere can be better simulated. We decided to increases the vertical resolution of the model by three times to match the fine resolution of 1.2 km used in the AER 2-D CTM. The model with finer resolution is running on a SGI machine. The results show some differences in the temperature fields between two versions of the model with different vertical resolution. The causes of the differences could be the scale dependent parameters in the dynamics module such as the sub-grid fourth order diffusion coefficients. We are adjusting these parameters to improve the model with finer vertical resolution.

The quasi-biennial oscillation (QBO) is the primary mode of variability in the tropical lower stratosphere and has been well documented (e. g. Reed et al., 1961). The QBO signals in the temperature have also been observed in the same area (e. g. Reed, 1964). Associated with the tropical temperature QBO anomalies is a meridianal circulation in the tropics and subtropics, which should have a direct effect on the tracer distribution in the lower tropic stratosphere. QBO signals in total ozone have been observed for over three decades (Funk and Garnham, 1962). The distributions of N_2O and CH_4 observed by UARS/HALOE also show QBO signals (Schoeberl, et al., 1997). In order to improve our model's ability to analyze the observed data or to use the model to assess atmospheric effects of pollutant, QBO should be included in the model. It is difficult for our 2-D interactive model to generate tropical waves to provide correct momentum sources for QBO due to the coarse vertical resolution and the simplified tropospheric dynamics. So instead, the zonal-mean QBO winds, averaged from NCEP data, are imposed on the model by adding a relaxation term in the zonal-mean zonal momentum equation. The time scale of relaxation is about 100 days. The model generates the right QBO in the zonal winds but

only a weak QBO signal in the temperature. Accordingly, the QBO signals in ozone and other tracers are small. We are analyzing the model outputs to diagnose the causes of the weak QBO signals in temperature.

(II. 2) Coupling of the 3-wave Model to the 2-D 19-Zone Climate Model

In order to examine the total effects of solar variation and stratospheric aerosols, including their indirect effects from changes in ozone, we are upgrading the 2-D climate-chemistry model (CCM). One of the refinements is to replace the 2-D dynamic-chemistry-transport module of the 2-D CCM with the 3-wave model (Shia et al, 1997), which resolves the three longest planetary waves and calculates the eddy diffusion coefficient for chemical tracers from the resolved planetary waves. Thus, the model includes more interactions between chemistry, radiation and dynamics. In addition, the 3-wave model has updated heterogeneous chemistry.

The new model is running well on a multi-processor SGI machine when the data exchange between the two modules, the 3-wave model and the climate model, is turned off. The next step is to establish full interactions between these two modules

(III) Assessment Related Activities

(III.1) Models and Measurements Workshop (II)

Our participation in the Models and Measurements Workshop has involved several of us at AER in different ways. Malcolm Ko contributed to the definition of one of the experiments. Courtney Scott is responsible for the analysis of the source gases experiment. The group, as a whole, has produced model results for the UADP archive. Malcolm Ko attended the first meeting in August and both Malcolm and Courtney attended the second meeting in November, 1997. At the meeting, Courtney made a presentation of the results from the source gases experiment. A write-up of the experiment was also submitted to UADP in January, 1998.

Malcolm Ko will also help co-ordinate the preparation of the final report.

(III.2) Ozone Assessment Report

Malcolm Ko is a co-author for Chapter 1 of the *WMO Ozone Assessment Report* with lead authors for the chapter, Ronald Prinn and Rudolf Zander. Chapter 1 deals with long-lived trace gases. Malcolm Ko worked with Michael Volk to prepare a section on the atmospheric lifetimes of the gases as can be determined from model calculations and observations. The model calculated lifetimes are taken from the Models and Measurements Workshop (II) calculations. The results from observations are taken from Volk et al. (JGR, 102, 25543, 1997) which uses historical records of tropospheric measurement to correct the observed correlation in the lower stratosphere to obtain steady state lifetimes. One result of the study is that there are indications that the lifetime of CFC-11 may be shorter than the currently accepted value of 50 years. A clearer picture should emerge when the uncertainty in the lifetime can be reduced.

Jose Rodriguez is lead author for Chapter 2 along with Michael Kurylo. Jose's effort is funded by this project. Chapter 2 deals with source gases that are removed by OH in the troposphere and a large part of the chapter was devoted to methyl bromine (CH_3Br), including its ozone depletion potential

We also performed some chlorine loading calculations and communicated our results to Guus Velder who is one of the lead authors of Chapter 11. Finally, results from a 1970-2050 trend calculation with the AER 2-D CTM were submitted to Chapter 12 by the January 1998 deadline. This calculation was performed with observed monthly mean temperatures and temperature probability distributions between 1979 and 1995.

(IV) Chlorine loading and stratospheric cooling

Recent winter/spring observations in the Arctic [Manney et al., 1996,1997; Müller et al., 1997; Rex et al., 1997] reveal further reductions of the ozone content despite nearly complete disappearance of Pinatubo aerosol from the stratosphere [Thomason et al., 1997] and essentially constant levels of chlorine and bromine loading [WMO, 1995]. Existing photochemical models of the stratosphere with heterogeneous chemistry predict little or no further stratospheric ozone depletion, unless an alternative mechanism is invoked. One such mechanism could be the cooling of the lower stratosphere [Oort and Liu, 1993; Randel and Cobb, 1994; Ramaswamy et al., 1996] leading to triggering of polar stratospheric cloud (PSC) formation. As a result, chlorine activation by enhanced PSCs provides further ozone decline during the winter/spring period. Here, we present sensitivity study results of the AER box model for typical conditions in the lower stratosphere at 70°N during the December 1 - April 1 period for an idealized parcel with different assumed stratospheric coolings and chlorine loadings. Our calculations show that the imposed

stratospheric cooling could further deplete ozone and retard its expected recovery even with the projected chlorine loading decrease. We show that, for the present conditions, a 1 K cooling could provide the same local ozone depletion as an increase of chlorine by 0.40-0.95 ppbv for the scenarios considered. Thus, sustained stratospheric cooling could further reduce Arctic ozone content and delay the anticipated ozone recovery in the Northern hemisphere even with the realization of the Montreal Protocol and its Amendments.

(V) The POLARIS Campaign

Malcolm Ko was in Fairbanks, Alaska for the deployment of the Polaris Campaign in July. Jose Rodriguez joined the September deployment, using the opportunity to meet with Michael Kurylo to work on Chapter 2 of the *WMO Ozone Assessment Report.*

One focus of the analysis continues to be the NO_x/NO_y ratio. The observed NO_x/NO_y is larger than that calculated using a constrained photochemical model. R.-S. Gao (NOAA) and Ross Salawitch (JPL) have tried to use a rate constant for OH + NO_2 that is 50% slower than the JPL recommendation. We used the AER 2-D CTM to perform some calculations to see its effect on model calculated ozone trends.

A copy of the manuscript is included as an appendix.

(VI) Anticipated Activities in the Next Six Months

Activities for the next six months will be dictated by the various assessment related activities of both the Models and Measurements Workshop, and of the WMO report. We hope to find time to revise some of our manuscripts for publications.

References:

Manney, G.L., M.L. Santee, L. Froidevaux, J.W. Waters, and R.W. Zurek, Polar vortex conditions during the 1995-96 Arctic winter: Meteorology and MLS ozone, *Geophys. Res. Lett.*, **23**, 3203-3206, 1996.

Manney, G.L., L. Froidevaux, M.L. Santee, R.W. Zurek, and J.W. Waters, MLS observations of Arctic ozone loss in 1996-97, *Geophys. Res. Lett.*, **24**, 2697-2700, 1997.

Müller, R. et al., Severe chemical ozone loss in the Arctic during the winter of 1995-96, *Nature*, **389**, 709-712, 1997.

Oort, A.H., and H. Liu, Upper-air temperature trends over the globe, *J. Climate*, **6**, 292-307, 1993.

Randel, W.J. and J.B. Cobb, Coherent variations of monthly mean total ozone and lower stratospheric temperature, *J. Geophys. Res.*, **99**, 5433-5447, 1994.

Ramaswamy, V., M.D. Schwartzkopf, and W.J. Randel, Fingerprint of ozone depletion in the spatial and temporal pattern of recent lower-stratospheric cooling, *Nature*, **382**, 616-618, 1996.

Rex, M., et al., Prolonged stratospheric ozone loss in the 1995-96 Arctic winter, *Nature*, **389**, 835-838, 1997.

Thomason, L.W., L.R. Poole, and T. Deshler, A global climatology of stratospheric aerosol surface area density deduced from SAGE II measurements: 1984-1994, *J. Geophys. Res.*, **102**, 8967-8976, 1997.

Volk, C.M., J.W. Elkins, D.W. Fahey, G.S. Dutton, J.M. Gilligan, M. Loewenstein, J.R. Podolske, K.R. Chen, and M.R. Gunson, Evaluation of source gas lifetimes from stratospheric observations, *J. Geophys. Res.*, **102**, 25543-25564, 1997

WMO Scientific Assessment of Ozone Depletion: 1994, World Meteorological Organization Global Ozone Research and Monitoring Project, Rep. 37, Geneva, Switzerland , 1995.

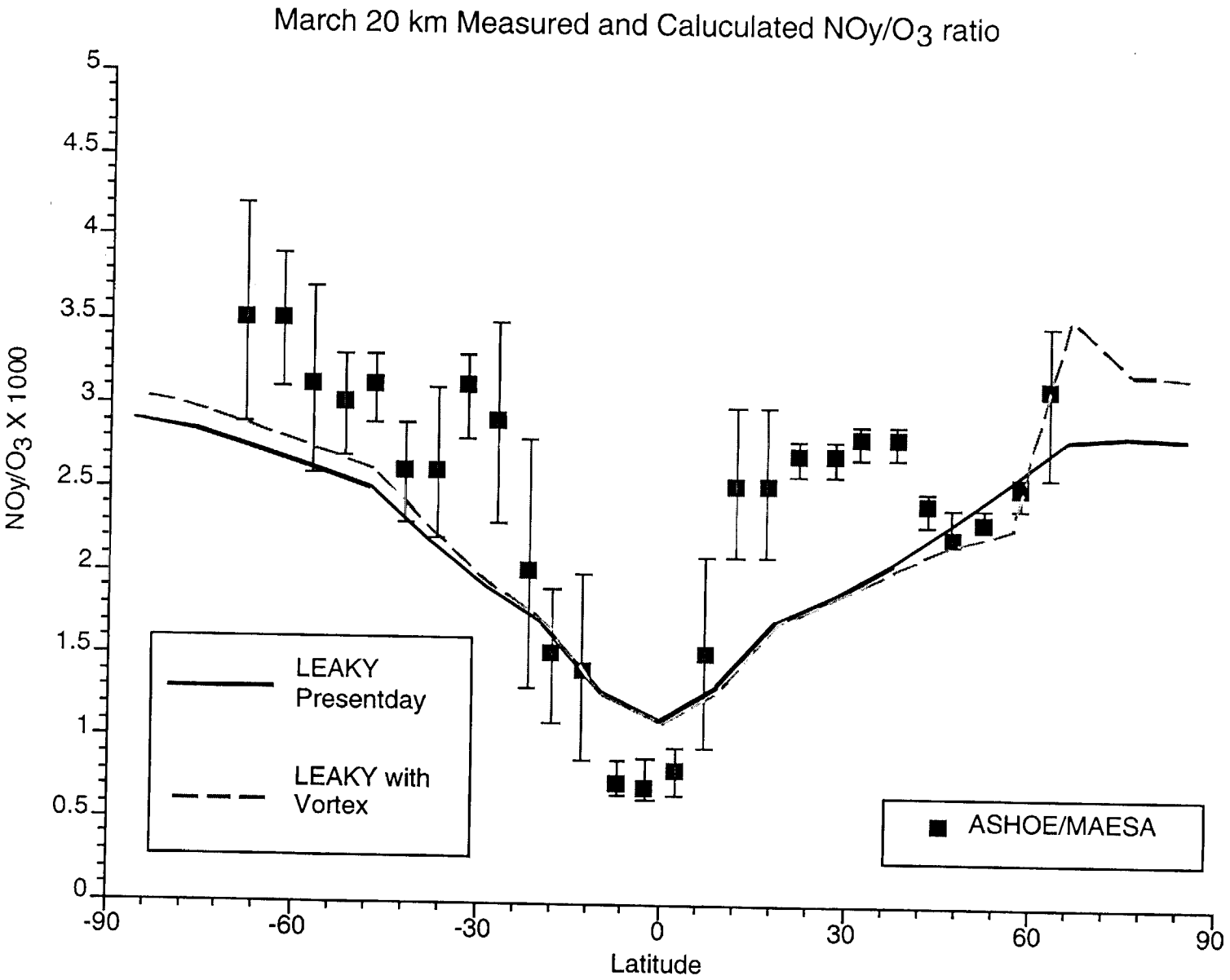
March 20 km Measured and Caluculated NOy/O3 ratio
NOy/O3 X 1000
5
4.5
4
3.5
3
2.5
2
1.5
1
0.5
0
-90
-60
-30
0
30
60
90
Latitude
LEAKY Presentday
LEAKY with Vortex
ASHOE/MAESA

1. AGENCY USE ONLY (Leave blank)	2. REPORT DATE	3. REPORT TYPE AND DATES COVERED
	March 13, 1998	Bi-annual July 1997 - December 1997

4. TITLE AND SUBTITLE

Coupling Processes between Atmospheric Chemistry and Climate

5. FUNDING NUMBERS

NAS5-97039

6. AUTHOR(S)

M.K.W. Ko, Debra Weinsenstein, Run-Li Shia, and N.D. Sze

7. PERFORMING ORGANIZATION NAME(S) AND ADDRESS(ES)

Atmospheric and Environmental Research, Inc.
840 Memorial Drive
Cambridge, MA 02139

8. PERFORMING ORGANIZATION REPORT NUMBER

P-698

9. SPONSORING/MONITORING AGENCY NAME(S) AND ADDRESS(ES)

NASA
Goddard Space Flight Center
Earth Sciences Procurement Office
Greenbelt, MD 20771

10. SPONSORING/MONITORING AGENCY REPORT NUMBER

11. SUPPLEMENTARY NOTES

12a. DISTRIBUTION/AVAILABILITY STATEMENT

12b. DISTRIBUTION CODE

13. ABSTRACT *(Maximum 200 words)*

This is the second semi-annual report for NAS5-97039. Work in this project is related to NAS1-20666, also funded by NASA ACMAP. The overall objective of this project is to improve the understanding of coupling processes between atmospheric chemistry and climate. Model predictions of the future distributions of trace gases in the atmosphere constitute an important component of the input necessary for quantitative assessments of global change. We will concentrate on the changes in ozone and stratospheric sulfate aerosol, with emphasis on how ozone in the lower stratosphere would respond to natural or anthropogenic changes.

The key modeling tools for this work are the AER two-dimensional chemistry-transport model, the AER two-dimensional stratospheric sulfate model, and the AER three-wave interactive model with full chemistry. We will continue developing our three-wave model so that we can help NASA determine the strength and weakness of the next generation assessment models.

14. SUBJECT TERMS

15. NUMBER OF PAGES

16. PRICE CODE

17. SECURITY CLASSIFICATION OF REPORT	18. SECURITY CLASSIFICATION OF THIS PAGE	19. SECURITY CLASSIFICATION OF ABSTRACT	20. LIMITATION OF ABSTRACT
Unclassified	Unclassified	Unclassified	

NASA
National Aeronautics and Space Administration

Report Documentation Page

1. Report No.	2. Government Accession No.	3. Recipient's Catalog No.

4. Title and Subtitle
Semi-Annual Report on Coupling Processes between Atmospheric Chemistry and Climate

5. Report Date
March 13, 1998

6. Performing Organization Code

7. Author(s)
M.K.W. Ko, Debra Weisenstein, Run-Li Shia, N.D. Sze

8. Performing Organization Report No.
P-698

10. Work Unit No.

9. Performing Organization Name and Address
Atmospheric and Environmental Research, Inc.
840 Memorial Drive
Cambridge, MA 02139

11. Contract or Grant No.
NAS5-97039

12. Sponsoring Agency Name and Address
NASA
Goddard Space Flight Center
Earth Sciences Procurement Office
Greenbelt, MD 20771

13. Type of Report and Period Covered
Bi-annual July '97-Dec.'97

14. Sponsoring Agency Code

15. Supplementary Notes

16. Abstract

This is the second semi-annual report for NAS5-97039. Work in this project is related to NAS1-20666, also funded by NASA ACMAP. The overall objective of this project is to improve the understanding of coupling processes between atmospheric chemistry and climate. Model predictions of the future distributions of trace gases in the atmosphere constitute an important component of the input necessary for quantitative assessments of global change. We will concentrate on the changes in ozone and stratospheric sulfate aerosol, with emphasis on how ozone in the lower stratosphere would respond to natural or anthropogenic changes.

The key modeling tools for this work are the AER two-dimensional chemistry-transport model, the AER two-dimensional stratospheric sulfate model, and the AER three-wave interactive model with full chemistry. We will continue developing our three-wave model so that we can help NASA determine the strength and weakness of the next generation assessment models.

17. Key Words (Suggested by Author(s))	18. Distribution Statement		
19. Security Classif. (of this report)	**20. Security Classif. (of this page)**	**21. No. of pages**	**22. Price**
Unclassified	Unclassified	11	

NASA FORM 1626 OCT 86

Appendix A

The Ozone Depletion Potential of CH_3Br

by

Malcolm K.W. Ko
Nien Dak Sze
Courtney Scott
José M. Rodriguez
Debra K. Weisenstein
Stan Sander[†]

January 1998

Submitted to JGR

Atmospheric and Environmental Research, Inc., Cambridge, MA
[†] Jet Propulsion Laboratory, Pasadena, CA.

Abstract

The ozone depletion potential (ODP) of methyl bromide (CH_3Br) can be determined by combining the model calculated ODP/BLP ratio (where BLP is the bromine loading potential) for CH_3Br and its atmospheric lifetime. This paper examines how changes in several key kinetic data affect the ODP/BLP ratio. The key reactions highlighted in this study include the reaction of $BrO + HO_2$, the absorption cross-section of HOBr, the absorption cross-section and the photolysis products of $BrONO_2$, and the heterogeneous conversion of $BrONO_2$ to HOBr and HNO_3 on aerosol particles. By combining the calculated ODP/BLP ratio with the latest estimate of 0.7 year for the atmospheric lifetime of CH_3Br, the likely value of ODP for CH_3Br is 0.39. The model calculated concentration of HBr (~ 0.3 pptv) in the lower stratosphere is substantially smaller than the reported measured value of about 1 pptv. The model can reproduce the measured value of 1.5 pptv if one assumes a yield for HBr of 1.3% from the reaction of BrO+OH, or a yield of 0.6% from the reaction of $BrO + HO_2$. Our calculations show that the effect of these assumed rates on the model calculated ODP/BLP ratio is minimal: practically no impact for the assumed BrO+OH yield and 10% smaller for the $BrO+HO_2$ case.

1. Introduction

Current measurements of the organic bromine compounds in the upper troposphere and lower stratosphere have confirmed that CH_3Br is the major contributor to stratospheric bromine loading (see e.g. Wamsley et al., 1998). The ozone depletion potential (ODP) of CH_3Br provides a measure of the expected effect on stratospheric ozone from emission of CH_3Br to the atmosphere. The ODP of CH_3Br is a function of the number of bromine radicals delivered to the stratosphere per unit mass of CH_3Br emitted at the ground and the ozone removal efficiency of the released bromine radicals. Analysis of the former is complicated by the large uncertainties associated with the atmospheric lifetime of CH_3Br. Apart from its removal by reaction with OH in the atmosphere, CH_3Br is also removed by deposition to soil and oceans. Although the impact of bromine chemistry on stratospheric ozone has been studied for close to two decades (see review in WMO, 1994), our knowledge of atmospheric bromine is still limited by the lack of direct observations of some of the bromine species in the stratosphere. With BrO being the only bromine species observed in aircraft campaigns, the type of process studies that can be used to verify our understanding of the partitioning in the atmosphere is limited. The recently reported measured HBr concentration of about 1 pptv (Nolt et al., 1997; Carlotti et al., 1995, Johnson et al., 1995; Park et al., 1989) in the lower stratosphere further complicated the picture as models are not able to reproduce this value with current rate data recommendations.

Changes in the values of the ODP of CH_3Br in the past have resulted from changes in both reaction rate constants for bromine radicals and changes in the atmospheric lifetime of CH_3Br. In this paper, we review how the calculated ODP for CH_3Br has changed with particular emphasis on the recent changes due to the revised rate constants in JPL-97 (DeMore et al., 1997).

2. ODP for CH_3Br

The Ozone Depletion Potential (ODP), first introduced by Wuebbles (1983), is now extensively used by policy makers as a simple relative measure to assess the potential impact of a given compound on the stratospheric ozone layer. The ODP is calculated relative to CFC-11 and depends principally on two major factors: a) the bromine loading potential (BLP) which measures the amount of bromine radicals delivered to the stratosphere per unit mass emitted at the ground, and b) the ODP/BLP ratio which measures the relative catalytic efficiency of the radicals in stratospheric ozone removal.

The bromine loading potential (BLP) reflects the amount of inorganic bromine added to the atmosphere from a given emission. An estimate for the amount of inorganic bromine present in the atmosphere due to the emission of a particular bromine-containing compound is given by the tropospheric concentration of the compound multiplied by the number of bromine atoms per molecule. At steady state (i.e., when additions to the atmosphere equal removal from the atmosphere), the estimate for the bromine concentration in parts per billion by volume (ppbv) is given by

$$[Br_y]_{ss_x} = E_{ss_x}\, \tau_x\, N_{Br}\, A_x$$

where N_{Br} is the number of halogen atoms per molecule of compound X, τ_x is the atmospheric lifetime of compound x, E_{ss_x} is the steady state emissions in mass per unit time and A_x is:

$$A_x = \frac{\mu_{air}}{\mu_x} * \frac{1}{\text{mass of the atmosphere}} * 10^9$$

where μ is molecular weight in grams, and the mass of the atmosphere is 4.8×10^{21} gm. The BLP is the ratio of the steady state concentration of bromine released by compound x for a given emission rate to the steady-state concentration of chlorine released by CFC-11 for an equal (by mass) emission rate:

$$BLP = \frac{\left[\frac{\tau N_{Br}}{\mu}\right]_x}{\left[\frac{\tau N_{Cl}}{\mu}\right]_{CFC\text{-}11}}.$$

The ODP is defined as the ratio of the ozone depletion produced by a unit-mass emission of compound X to the ozone depletion produced by a unit-mass emission of CFC-11 (the traditional reference gas). Numerical models that incorporate the pertinent chemistry and trace gas transport of the atmosphere are used to compute the ODP. For such modeling exercises, the steady state ODP for compound X can be given by (Fisher et al., 1990):

$$ODP = \frac{\dfrac{\textit{calculated steady state ozone depletion of about 1\% due to X}}{\textit{emission rate of X to produce this decrease of ozone in the model}}}{\dfrac{\textit{calculated steady state ozone depletion of about 1\% due to CFC-11}}{\textit{emission rate of CFC-11 to produce this decrease of ozone in the model}}}$$

where 1% depletion is required to yield results above model noise levels but within the region of linear model response. The ratio BEF_X, defined by $\left[\frac{ODP}{BLP}\right]_X$ is a measure of the relative ozone removal efficiency of the bromine radicals delivered to the stratosphere. In the definition, the behavior of CFC-11 is used as the reference standard. The value of BEF corresponds to the spatial and seasonal average of the local ozone removal efficiency of the bromine radicals released by X relative to the chlorine atoms released by CFC-11. Note that the BEF value is species dependent, i. e., if two species release bromine radicals at different locations in the lower stratosphere, the BEF values will be different for the two species.

Because of differences in model formulation, different models will calculate slightly different atmospheric lifetimes. This is further complicated by the fact that some species are affected by surface removal processes that are difficult to model. Previous analyses (see e.g. Solomon et al., 1992) have shown that the model calculated ODP/BLP ratio depends on the local stratospheric lifetime of the source gas. Changes in lifetimes due to tropospheric and surface processes would not affect the ODP/BLP ratio as long as they are not so fast that the mixing ratio of the source gas becomes non-uniform in the troposphere. Making use of this property, one can define the ODP and BLP using the standard recommended lifetime (τ_{rec}) as follows. The model is used to calculate atmospheric lifetime (τ_{model}) and $(ODP)_{model}$ according to its definition, taking care that all the stratospheric processes are properly accounted for. A value for $(BLP)_{model}$ is then defined as

$$(BLP)_{model} = \frac{\left[\frac{N_{Br}}{\mu}\right]_x}{\left[\frac{N_{Cl}}{\mu}\right]_{CFC\text{-}11}} \frac{\left[\tau_{model}\right]_x}{\left[\tau_{model}\right]_{CFC\text{-}11}}$$

and the model calculated BEF_x is given by

$$BEF_X = \frac{(ODP)_{model}}{(BLP)_{model}}$$

The ODP value based on the recommended lifetime is defined as

$$(\mathrm{ODP})_{\tau rec} = (\mathrm{BLP})_{\tau rec} \frac{(ODP)_{model}}{(BLP)_{model}} = (\mathrm{BLP})_{\tau rec}\, \mathrm{BEF}_x$$

where $(\mathrm{BLP})_{\tau rec}$ is defined as

$$(\mathrm{BLP})_{\tau rec} = \frac{\left[\frac{N_{Br}}{\mu}\right]_x}{\left[\frac{N_{Cl}}{\mu}\right]_{CFC\text{-}11}} \frac{\left[\tau_{rec}\right]_x}{\left[\tau_{rec}\right]_{CFC\text{-}11}}$$

and τ_{rec} is determined through consensus of the modeling community.

Table 1 summarizes how the calculated values of ODP for CH_3Br has changed since 1990. These values are calculated by the AER model using different rate constants as available at the time. Between 1990 and 1997, the BEF for CH_3Br has increased while its lifetime has decreased. On balance, the ODP has decreased from 0.99 to 0.39.

3 Atmospheric Lifetime of Methyl Bromide

The net atmospheric lifetime (τ_{tot}) for methyl bromide is given by:

$$\frac{1}{\tau_{tot}} = \frac{1}{\tau_{gas}} + \frac{1}{\tau_{ocean}} + \frac{1}{\tau_{land}}$$

In the above expression, τ_{gas} denotes the lifetime against atmospheric removal by gas-phase reactions and photolysis of CH_3Br, and is defined by the total column density (cm^{-2}) divided by the integrated loss rate ($cm^{-2}s^{-1}$) over the whole atmosphere. The lifetime against ocean uptake, τ_{ocean}, is defined as the methyl bromide atmospheric burden divided by the flux into the ocean. A similar definition holds for the lifetime against uptake by land surfaces, τ_{land}.

Although photolysis and reactions of CH_3Br with $O(^1D)$, $O(^3P)$, NO_3, and Cl take place in the atmosphere, gas-phase removal of methyl bromide is likely to be dominated by its reaction with tropospheric OH. Based on the latest recommended rate constants of the reaction of CH_3Br with OH, and of CH_3CCl_3 with OH, together with the most recent analysis of ALE/GAGE data (Prinn et al., 1995), a partial lifetime due to reaction with OH in the troposphere for CH_3Br of 2.1 ± 0.5 years, is derived. When combined with the partial lifetime due to stratospheric removal, the estimated τ_{gas} is 1.7 years.

Hydrolysis and reaction with chloride ions in sea water constitute an important sink for atmospheric CH_3Br. This is in contrast to halocarbons and proposed substitutes which, due to low solubility (typically $H \sim 10^{-2}$ moles/l/atm)and aqueous degradation rates (typically $k_w \sim$

10^{-9} s^{-1}), have ocean uptake lifetimes of order of hundreds of years (Wine and Chameides, 1990). Butler (1994) described a method to calculate the (partial) atmospheric lifetime of CH_3Br due to removal by the ocean (τ_{ocean}) in terms of the surface mixed layer depth of the ocean, sea-surface temperature, wind speed, thermocline diffusivity, solubility of CH_3Br in sea water, and degradation rate coefficient in sea water. The Butler (1994) estimate was carried out using a two-box model so that weighted averages of the parameters were used in the calculations. The calculated best estimate for τ_{ocean} was 3.7 years, with a possible range from 1.4 year to 14 years. These values were adopted in the WMO 1994 report. The same methodology was used in Yvon and Butler (1996) but with the parameters calculated individually for each 2° by 2° grid over the oceans. Thus, they were able to take into account the co-variations of the parameters before summing the effects to obtain the global partial lifetime. With this method, they obtained a best estimate for τ_{ocean} of 2.7 years, with a range from 2.4 years to 6.5 years. The latest update (Yvon-Lewis and Butler, 1997) includes biological removal and lowers the lifetime to 1.8 years, with a range from 1.1 years to 3.9 years.

Measurements of deposition velocity of CH_3Br over land are not available. Based on the uptake rates measured for five types of soil, Shorter et al. (1995) computed the partial lifetime of CH_3Br. The value is based on the sum of the annual uptake fluxes (g yr^{-1}) by the five soil types, each of which is estimated as the product of the uptake rate for the soil type (g m^{-2} d^{-1}), the area of the soil type on the globe (m^2), and the number of active days in a year (d yr^{-1}). The five soil types were assigned two uptake rates, corresponding to deposition velocities of 0.12 cm s^{-1} and 0.02 cm s^{-1}. The value obtained due to soil removal is 3.4 years.

Combining the three partial lifetimes provides a best estimate of 0.7 years.

4 Partitioning of the Bromine Radicals

We used the AER 2-D model (Weisesntein et al., 1996) with the standard JPL reaction rate constants for the gas-phase reactions and parameterization for heterogeneous reactions on sulfate aerosol. Following the method used in WMO (1992), the ODP is calculated based on a background chlorine and bromine concentration of 3.5 ppbv and 19 pptv, respectively.

The concentrations of the bromine radicals at 38°N for spring conditions calculated using JPL-97 recommended rate constants are shown in figure 1. Note that at that latitude, $BrONO_2$ and BrO are the most abundant species. The concentrations of HOBr and HBr are less than 1 pptv. Figures 2a and 2b show the computed [BrO]/[Br_y] ratio along with observations reported by Avalonne et al. (1995). It is evident that the BrO concentrations calculated using JPL-97 are larger than those calculated using JPL-94. This accounts for the larger BEF in Table 1.

The reported measured concentration of 1.5 pptv for HBr between 25 and 35 km (Carlotti et al., 1996) is much larger than the model computed value of about 0.3 pptv. In section 6, we will discuss ways of increasing the calculated concentration of HBr in the model and how they affect BEF.

5. Sensitivity of BEF to Rate Data

The following reactions represent the primary bromine-driven catalytic ozone removal cycles in the stratosphere:

$$\begin{aligned} ClO + BrO + h\nu &\rightarrow Br + Cl + O_2 \\ Br + O_3 &\rightarrow BrO + O_2 \\ Cl + O_3 &\rightarrow ClO + O_2 \end{aligned} \qquad \text{(I)}$$

$$ClO + BrO + h\nu \rightarrow Br + Cl + O_2$$
$$Br + O_3 \rightarrow BrO + O_2$$
$$Cl + O_3 \rightarrow ClO + O_2 \qquad \text{(I)}$$

$$2O_3 \rightarrow 3O_2.$$

$$\left.\begin{aligned} BrO + HO_2 &\rightarrow HOBr + O_2 \\ HOBr + h\nu &\rightarrow OH + Br \\ Br + O_3 &\rightarrow BrO + O_2 \\ OH + O_3 &\rightarrow HO_2 + O_2 \end{aligned}\right\} \qquad \text{(II)}$$

$$2O_3 \rightarrow 3O_2.$$

$$\left.\begin{aligned} BrO + O &\rightarrow Br + O_2 \\ Br + O_3 &\rightarrow BrO + O_2 \end{aligned}\right\} \qquad \text{(III)}$$

$$O + O_3 \rightarrow 2O_2.$$

$$\left.\begin{aligned} 2(Br + O_3 &\rightarrow BrO + O_2) \\ BrO + BrO &\rightarrow 2Br + O_2 \end{aligned}\right\} \qquad \text{(IV)}$$

$$2O_3 \rightarrow 3O_2.$$

and

$$\left.\begin{aligned} BrNO_3 + h\nu &\rightarrow Br + NO_3 \\ NO_3 + h\nu &\rightarrow NO + O_2 \\ Br + O_3 &\rightarrow BrO + O_2 \\ NO + O_3 &\rightarrow NO_2 + O_2 \\ BrO + NO_2 + M &\rightarrow BrNO_3 + M \end{aligned}\right\} \qquad \text{(V)}$$

$$2O_3 \rightarrow 3O_2.$$

Current rate constants indicate that, in the present day atmosphere, the first three cycles contribute about an equal amount to ozone depletion in the lower stratosphere, with the last two about an order of magnitude smaller.

To illustrate how changes in rate constants affect BEF, we summarize the key revisions between the JPL-94 and JPL-97 in Table 2. Changes to reactions (R1) through (R8) (see Table 2) impact the ozone removal efficiency either directly because they are the rate limiting step in the cycle, or indirectly by changing the partitioning between BrO and the reservoir species. We explore the dependence by performing a series of calculations to obtain the BEF in each case. The results are summarized in Table 3.

Reaction R1 in Table 2 has received much attention. A key revision in JPL-92 that affects the BEF value for CH_3Br is the faster rate constant for reaction of BrO and HO_2. With an estimated temperature dependence, the rate recommended in JPL-92 based on room temperature value by Poulet et al. (1992) is about a factor of 10 faster at stratospheric temperatures than that recommended by JPL (1990). Reaction R1 represents the rate limiting steps in cycle (II). With the rate constant from JPL-92 (a ten-fold increase compared to JPL-90), the BEF increases from 37 to 49.

In the JPL-94 calculation, we included the absorption cross-section for HOBr as reported by Orlando and Burkholder (1995), which is the first measured absorption cross-section. Prior to that, the much larger cross-section of HOCl was used as a proxy, resulting in computed HOBr concentration of less than 0.1 pptv at 16 km and 0.8 pptv at 30 km. With the Orlando and Burkholder cross-section, the concentration of HOBr is around 1 pptv at 16 km and 3 pptv around 30 km (see the curve labeled JPL-94 in Figure 3), comparable to those of BrO and $BrONO_2$. Inclusion of this cross-section lowers the BEF from 49 to 44.

Several revisions in JPL-97 identified in Table 2 also have impacts on the model calculated HOBr. A smaller rate constant for R1 results in smaller HOBr (see Case B in Figure 3). The heterogeneous reaction R3 convert $BrONO_2$ to HOBr and BrO. As a result of this reaction, both HOBr and BrO are larger (see Case D in Figure 3). The combined effect of R1

and R3 is represented in Figure 3 as Case E. For comparison, we performed Case F where we have updated all the JPL-97 rate data except the absorption cross-sections. The value obtained in the lower stratosphere is similar to Case E. The difference between Case E and Case F around 30 km is the result of the slower rate for R8 (O + HOBr) in the JPL-97 recommendation. Figure 4 shows the absorption cross-section of HOBr from Orlando and Burkholder (1995) and the JPL-97 recommendation. As noted in JPL-97, the recommended cross-section is influenced by the measurements reported by Rattigan et al. (1996). With the larger cross-section between 300 nm and 400 nm and the extension of the cross-section beyond 400 nm, the photolysis rate of HOBr is three times larger in the lower stratosphere leading to a smaller concentration of HOBr (see cases F and JPL-97 in Figure 3).

We will now discuss the effects of the rate revisions on the model calculated BEF for CH_3Br. The Orlando and Burkholder cross-section decreases the sensitivity of the model calculated BEF to changes in the reaction rate constant for reaction (1). With HOBr being a major reservoir, any increase (decrease) in k_1 is compensated by decrease (increase) in [BrO] so that the change in the rate limiting step $k_1[BrO][HO_2]$ will be smaller than the corresponding change in k_1. This is illustrated by the results for case B in Table 3. Despite a factor of two decrease in the rate constant for R1, the ODP for case B is practically the same as that for case A. Revision of the $BrONO_2$ cross-section involves both the magnitude and the product yield. The measurement reported by Burkholder et al. (1995) extends the measured values to beyond 390 nm. With the new cross-section, the photolysis rate is a factor of 1.25 larger in the lower stratosphere. For $BrONO_2$ photolysis (R2), only $\Phi_{Br + NO3}$ leads to ozone destruction as the $\Phi_{BrO+NO2}$ branch is a null cycle. Previously, it has been assumed that $\Phi_{Br + NO3} = 1$ with $\Phi_{BrO + NO2} = 0$. The new values from Nickolaisen and Sander (private communication) indicate that $\Phi_{Br+NO3} = 0.29$ with $\Phi_{BrO+NO2} = 0.71$. Thus the new branching should decrease BEF. However,

diagnostics reveals that the cycle (V) contribution is small compared to the other cycles around 20 km. Thus, the effect of the change in branching on BEF is small as illustrated by Case C. However, the expected effect from the extension of the absorption cross-section to longer wavelength is to suppress $BrONO_2$ and increase BrO and BEF (see Case F and Case H).

Reaction (R3) is a major source of HO_x in the lower stratosphere via production of HOBr and its subsequent photolysis. The reaction also leads to a higher concentration of BrO and smaller concentration of NO_x. The smaller NO_x provides the coupling to the ClO_x and HO_x cycles. Cases D shows a 19% increase in the BEF. Our diagnostics reveal increased contributions from cycles (I) and (II) where a larger reservoir of HOBr and BrO are produced via reaction (R3).

The combined effects of R1, R2b and R3 is given in case E. The resulted BEF can be compared with that for Case F, which consists of all JPL-97 updates except the cross-sections. The similarrity in BEF for the two cases shows that the effects of R5 through R8 on BEF are small. The final four cases in Table 3 illustrate the contributions of the revisions the cross-sections on BEF. The HOBr revision has the largest effects among the revisions. The larger cross-section leads to larger calculated concentrations of BrOand larger BEF. For $BrONO_2$, the revision to the absorption cross-section again leads to a repartioning of the bromine radicals leading to higher concentrations of BrO. The effect from the change in branching is small. The cross-section revisions for $ClONO_2$ and BrCl are each responsible for increasing the BEF by 0.5 to bring the BEF to 58 in Case J.

6. The ODP and the BEF of CH_3Br with HBr concentrations at 1.5 pptv

The calculated concentration of HBr in Figure 1 is much smaller than values reported in the literature. To obtain calculated concentrations of HBr similar to recent measured values of HBr in the lower stratosphere by Carlotti et. al. (1995) and Nolt et al. (1997), we have to invoke alternative mechanisms to produce HBr.

Several studies (Larichev et al., 1995; Mellouki et al., 1994) indicated that the product of R1 is HOBr and O_2, although it is not possible to confirm or refute a small yield of HBr by direct measurements. Another possibility is a small yield of HBr from the reaction of BrO with OH. Two recent publications presented model results to show how a small yield from BrO + OH (Chipperfield et al., 1997) or yields from either reactions (Chartrand and McConnel, 1998) could successfully simulate the measured concentration. In two separate cases, we assume a 1.3% yield of HBr from BrO + OH, or an HBr yield of 0.6% from BrO + HO_2. Annual averages of HBr between 25 and 35 km are calculated to be 1.3 pptv and 1.5 pptv for the two cases respectively (see figure 5). In both cases, HBr is elevated by over 100% from Case A. The concentrations of the remaining bromine species are decreased by up to 10%. The effect on BEF is small as evident from the small changes in BrO in figure 6. The calculated BEF values are 56 (for the BrO +OH case) and 52 (for the BrO + HO_2) case, compared to a value of 58 calculated with no assumed HBr yield.

6. Concluding Remarks

The calculated ODP for CH_3Br depends not only on stratospheric bromine chemistry, but also on the calculated atmospheric lifetime. Some of the processes which define the surface removal are not yet well understood. In contrast to the vast amount of data on ClO_x species, observations of BrO_x species are few. Although observations of BrO in the lower stratosphere and the tentative upper limits on HBr above 30 km place some constraints on bromine chemistry, they do not rule out models which assume a small (5-10%) HBr branching. Laboratory studies of reactions (1) and (2) together with selective (but more frequent) stratospheric measurement (e.g., simultaneous measurement of BrO and HBr over an extended (20-30 km) altitude region) will help accelerate our understanding of stratospheric bromine chemistry.

Acknowledgments

Work supported by the Methyl Bromide Global Coalition and by the National Aeronautics and Space Administration (NASA) Atmospheric Chemistry Modeling and Analysis Program (ACMAP). The authors benefited from numerous discussions with participants at the Methyl Bromine State of the Science Workshop, 1997. Their contributions are gratefully acknowledged.

References

Avalone, L.M., D.W. Toohey, S.M. Schauffler, W.H. Polloack, L.E. Heidt and E.L. Atlas, In situ measurements of BrO during AASE II,. . *Geophysical Research Letters* , 22, 831-834, 1994., 1995

Burkholder, J.B., A.R. Ravishankara, and S. Solomon, UV/visible and IR absorption cross-section of $BrONO_2$, *J. Geophys. Res.*, 100, 16793-16800, 1995.

Butler, J.H., The potential role of the ocean in regulating atmospheric CH_3Br. *Geophysical Research Letters* , 21, 185-188, 1994.

Carlotti, M. et al., Measurement of stratospheric HBr using high resolution far infrared spectroscopy, *Geophys. Res. Lett.*, 22, 3207-3210, 1995.

Chartrand, D.J., and J.C. McConnell. Evidence for HBr production due to minor channel branching at mid-latitudes, *Geophys. Res. Lett.*, 25, 55-58, 1998.

Chipperfield, M.P., D.E. Shallcross, and D.J. Lary, A model study of the potential role of the reaction BrO + OH in the production of stratospheric HBr, *Geophys. Res. Lett.*, 24, 3025-3028, 1997.

Fisher, D.A., C.H. Hales, D.L. Filkin, M.K.W. Ko, N.D. Sze, P.S. Connell, D.J. Wuebbles, I.S.A. Isaksen and F. Stordal, Model calculations of the relative effects of CFCs and their replacements on stratospheric ozone. *Nature*, 344, 508-512, 1990.

JPL-94 (Jet Propulsion Laboratory), W.B. DeMore, D.M. Golden, R.F. Hampson, M.J. Kurylo, C.J. Howard, A.R. Ravishankara, C.E. Kolb, and M.J. Molina (1994) *Chemical Kinetics and Photochemical Data for Use in Stratospheric Modeling*. Evaluation No. 11, JPL Publication 94-26.

JPL-97 (Jet Propulsion Laboratory), W.B. DeMore, D.M. Golden, R.F. Hampson, M.J. Kurylo, C.J. Howard, A.R. Ravishankara, C.E. Kolb, and M.J. Molina (1997) *Chemical Kinetics and Photochemical Data for Use in Stratospheric Modeling*. Evaluation No. 12, JPL Publication 97-4.

Johnson, D.G., W.A. Traub, K.V. Chance, and K.W. Jucks, Detection of HBr and upper limits for HOBr: Bromine partitioning in the stratosphere, *Geophys. Res. Lett.*, 22, 1373-1376, 1995.

Larichev, M., F. Maguin, G. Le Bras, and G. Poulet, Kinetics and mechanism of $BrO+HO_2$ reaction, *J. Phys. Chem.*, 99, 15911-15918, 1995.

Mellouki, A., R.K. Talukdar, and C.J. Howard, Kinetics of the reactions of HBr with O_3 and HO_2: The yield of HBr from HO_2 + BrO, *J. Geophys. Res.*, 99, 22949-22954, 1994.

Nolt, I.G. et al., Styratospheric HBr concentration profile from far-infra-red emission spectroscopy, *Geophys. Res. Lett.*, 24, 281-284, 1997.

Orlando, J.J. & J.B. Burkholder, Gas phase UV/visible absorption spectra of HOBr and Br_2O, *J. Phys. Chem.*, 99, 1143, 1995.

Park, J.H., B. Carli, and A. Barbis, Stratospheric HBr mixing ratio obtained from far infrared emission spectra, *Geophys. Res. Lett.*, **16**, 787, 1989.

Poulet, G., M. Pirre, F. Maguin, R. Ramaroson, and G. LeBras, Role of the BrO + HO_2 reaction in the stratospheric chemistry of bromine. *Geophys. Res. Lett.*, **19**, 2305-2308, 1992

Prinn, R. T. , R.F. Weiss, B.R. Miller, J. Huang, F.N. Alyea, D.M. Cunnold, P.B. Fraser, D.E. Hartley, and P.G. Simmonds, Atmospheric trends and lifetime of trichloroethane and global average hydroxyl radical concentrations based on 1978-1994 ALE/GAGE measurements. *Science* 269, 187-192, 1995.

Rattigan, O., D.J. Lary, R.L. Jones, and R.A. Cox, UV-visible absorption cross-section of gaseous Br_2O and HOBr, *J. Geophys. Res.*, **101**, 23021-23033, 1996.

Shorter, J.H., C.E. Kolb, P.M. Crill, R.A. Kerwin, R.W. Talbot, M.E. Hines, and R.C. Harriss, Rapid degradation of atmospheric methyl bromide in soils. *Nature* 377 (6551):717-719, 1995.

Solomon,S., M. Mills, L.E. Heidt, W.H. Pollock, and A.F. Tuck, On the evaluation of ozone depletion potentials, *J. Geophys. Res.*, **97**, 825-842, 1992.

Wamsley P.R., J.W. Elskins, D.W. Fahey, G.S. Dutton, C.M. Volk, R.C. Myers, S.A. Montzka, J.H. Butler, A.D. Clarke, P.J. Fraser, L.P. Steele, M.P. Lucarelli, E.L. Atlas, S.M. Schauffler, D.R. Blake, F.S. Rowland, R.M. Stimpfle, K.R. Chan, D.K. Weisesntein, and

M.K.W. Ko (1997), Distribution of upper tropospheric and lower stratospheric halon-1211 and the 1994 bromine budget, *J. Geophys Res.*, **103D**, 1513-1526, 1998.

Weisenstein, D.K., M.K.W. Ko, N-D Sze, and J.M. Rodriguez, Potential impact of SO_2 emissions from stratospheric aircraft on ozone. *Geophys. Res. Lett.*, **23**, 161-164, 1996.

Wine, P.H., and W.L. Chameides, Possible atmospheric lifetimes and chemical reaction mechansim for selected HCFCs, HFCs, CH_3CCl_3, and their degradation products against dissolution and/or degradation in seawater and cloud water, in *Scientific Assessment of Startospheric Ozone: 1989*. Volume II, World Meteorological Organization Report No. 20. Geneva, Switzerland, 1990.

Wuebbles, D.J., Chlorocarbon emission scenarios: potential impact on stratospheric ozone. *J. Geophys. Res.*, **88**, 1433, 1983.

World Meteorological Organization (WMO) (1992) *Scientific Assessment of Ozone Depletion: 1991*. World Meteorological Organization Report No. 25. Geneva, Switzerland, 1992.

World Meteorological Organization (WMO) (1994) *Scientific Assessment of Ozone Depletion: 1994*, World Meteorological Organiziation Global Ozone Research and Monitoring Project, report No. 37. Geneva, Switzerland, 1995.

Yvon, S.A., and J.H. Butler, An improved estimate of the oceanic lifetime of atmospheric CH_3Br, *Geophysical Research Letters* 23 (1):53-56, 1996.

Yvon-Lewis, S.A., and J.H. Butler, The potential effect of oceanic biological degradation on the lifetime of atmospheric CH_3Br. *Geophysical Research Letters* 24 (10), 1227-1230, 1997.

Figure Captions:

Figure 1: Model calculated day-time averaged mixing ratio profiles for spring conditions at 38°N latitudes. The calculations were performed using JPL-97 rate recommendations.

Figure 2a: Comparison of model calculated values of the BrO/Bry ratio compared with the values derived from the AASE-II measurements as reported by Avalone et al. (1995). The model values are for 20 km altitude and are taken from the 2-D CTM computed using model calculated values of BrY and ozone. The results are sorted by latitudes.

Figure 2b: Same as figure 2a except that the results are sorted by solar zenith angles.

Figure 3: Model calculated day-time average concentration of HOBr for different cases. See Table 3 for the description of the cases.

Figure 4: Absorption cross-sections of HOBr from Orlando and Burkholder (1995) and the JPL-97 recommendation.

Figure 5: Model calculated mixing ratio profiles for HBr calculated using JPL-94 and JPL-97 rate data recommendations. The curve labeled BrO + OH is calculated assuming an HBr yield of 1.3% from the reaction. The curve labeled BrO + HO2 assumes an HBr yield of 0.6% from the reaction.

Figure 6: Same as figure 5 except for BrO.

Table 1: Values of ODP for CH_3Br

circa	BEF	key revision	τ_{rec} (years)	comment	ODP
1992	36	-	2.1	removal by OH only	0.73
1992	49	$BrO+HO_2$ 10 times faster	2.1	removal by OH only	0.99
1994	48	JPL-94	1.3	include removal by ocean	0.60
1994	44	HOBr cross-section from Orlando and Burkholder (1995)	1.3	include removal by ocean	0.55
1997	58	see table 2	0.7	include removal by soil, and biological removal in ocean water	0.39

Table 2: Summary of rate revisions for key bromine chemistry reactions in JPL-97

rate	JPL-97	JPL-94	remark
R1: $BrO + HO_2$	$3.4\times10^{-12}\exp(540/T)$	$6.2\times10^{-12}\exp(500/T)$	new rate is 0.65 times old rate @ 230K
R2a: absorption cross-section of $BrONO_2$,	temperature dependent cross-section extended to longer wavelengths		new J rate is 1.25 times larger than the old one
R2b: quantum yield	$\Phi_{BrO+NO2} = 0.71$, $\Phi_{Br+NO3} = 0.29$	$\Phi_{BrO+NO2} = 0$ $\Phi_{Br+NO3} = 1.0$	cyle V is 0.3 times smaller
R3: heterogeneous conversion of $BrONO_2$ on sulfate	temperature dependent rate with γ as large as 0.8	no recommendation	
R4: photolysis of HOBr,	larger cross-section at long wavelengths,		new J rate is a factor of three larger than old
R5: BrO + O	$1.9\times10^{-11}\exp(230/T)$	$1.7\times10^{-11}\exp(260/T)$	new rate 0.98 times old rate @ 230K
R6: BrO + BrO	$1.5\times10^{-12}\exp(230/T)$	$4.0\times10^{-12}\exp(-190/T)$ $4.2\times10^{-14}\exp(660/T)$	new rate is 1.6 times old rate @ 230K
R7: BrO + OH	7.4×10^{-11}	1×10^{-11}(estimated)	
R8: O + HOBr	$1.2\times10^{-10}\exp(-430/T)$	2.5×10^{-11} (@298K)	

Table 3: Model calculated BEF using different input

	comment	BEF
case A	JPL-94*	44
case B	JPL-94* + R1	43
case C	JPL-94* + R2b	43
case D	JPL-94* + R3	54
case E	JPL-94* + R1 +R2b + R3	49
case F	JPL-97 except all photolysis absorption cross sections are from JPL-94	49
case G	case F + HOBr cross-section from JPL-97	54
case H	case F + $BrONO_2$ cross-section from JPL-97	52
case I	case F + HOBr and $BrONO_2$ cross-section from JPL-97	57
case J	JPL-97	58

* use Orlando and Burkholder (1995) cross-section for HOBr

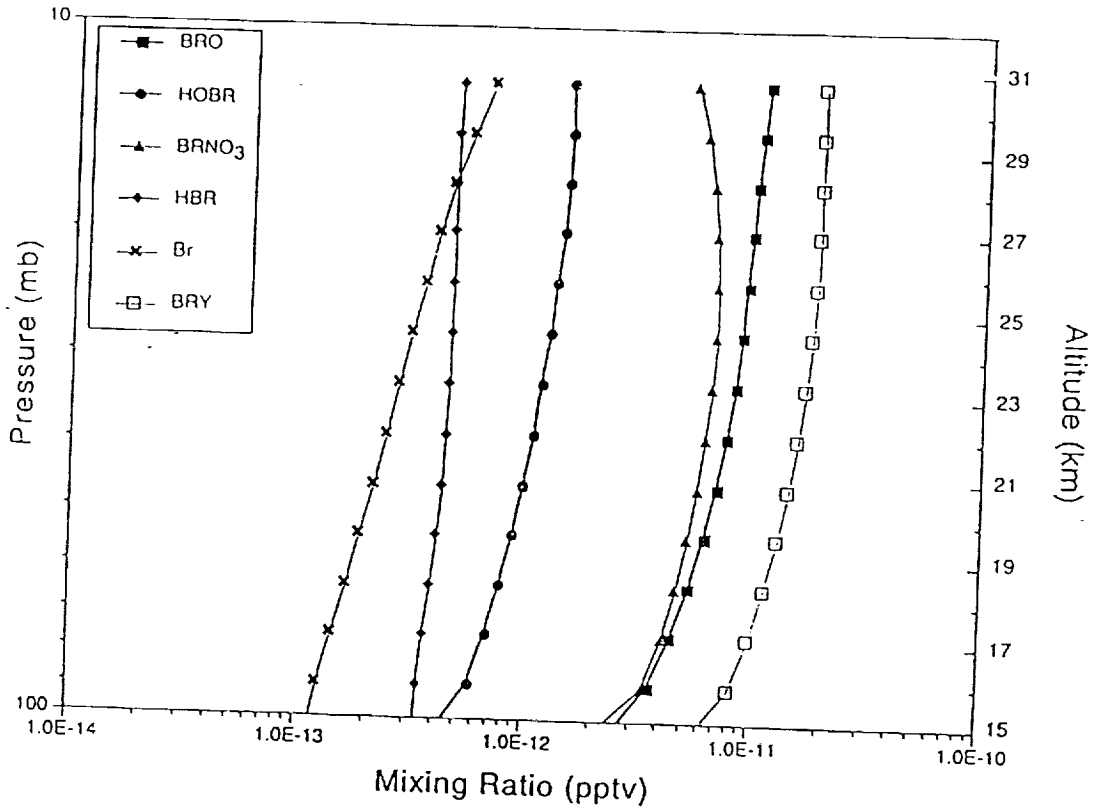

Figure 1: Model calculated day-time averaged mixing ratio profiles for spring conditions at 38°N latitudes. The calculations were performed using JPL-97 rate recommendations.

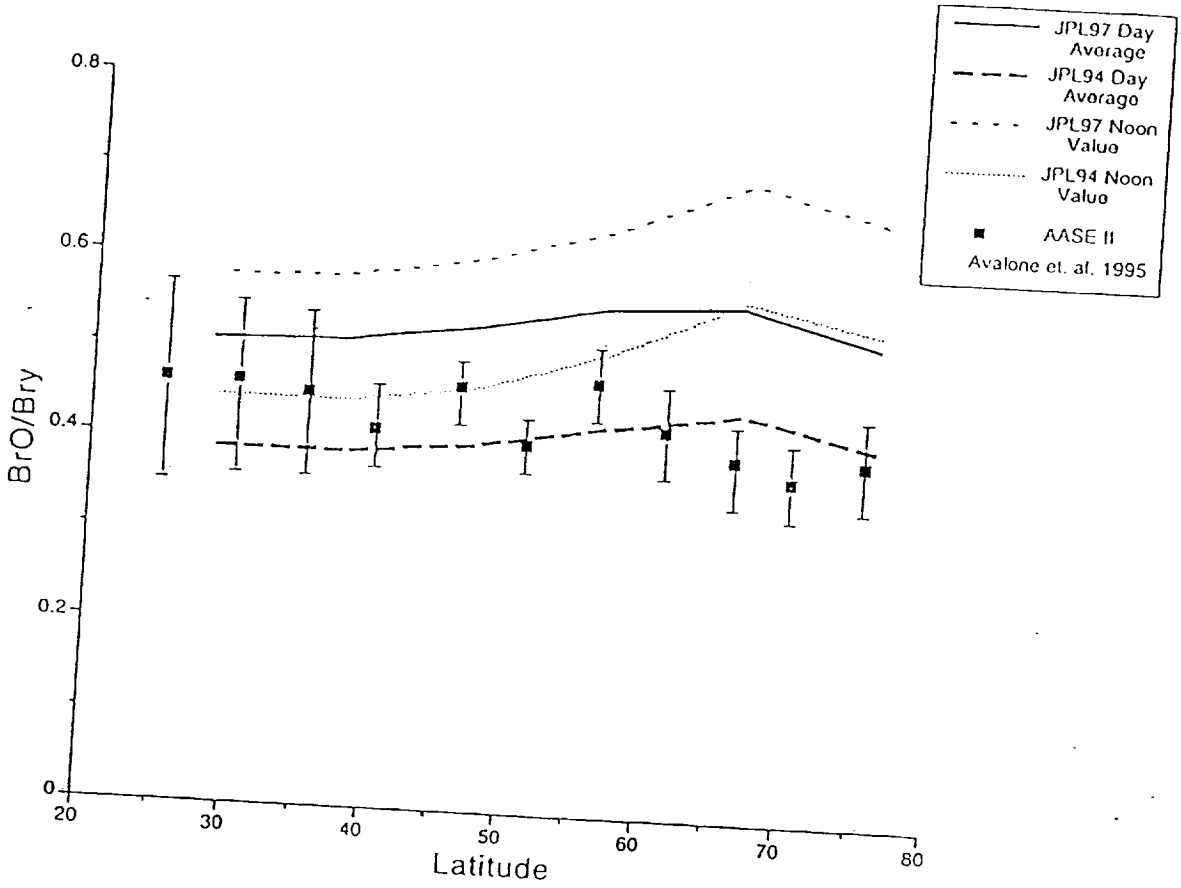

Figure 2a: Comparison of model calculated values of the BrO/Bry ratio compared with the values derived from the AASE-II measurements as reported by Avalone et al. (1995). The model values are for 20 km altitude and are taken from the 2-D CTM computed using model calculated values of BrY and ozone. The results are sorted by latitudes.

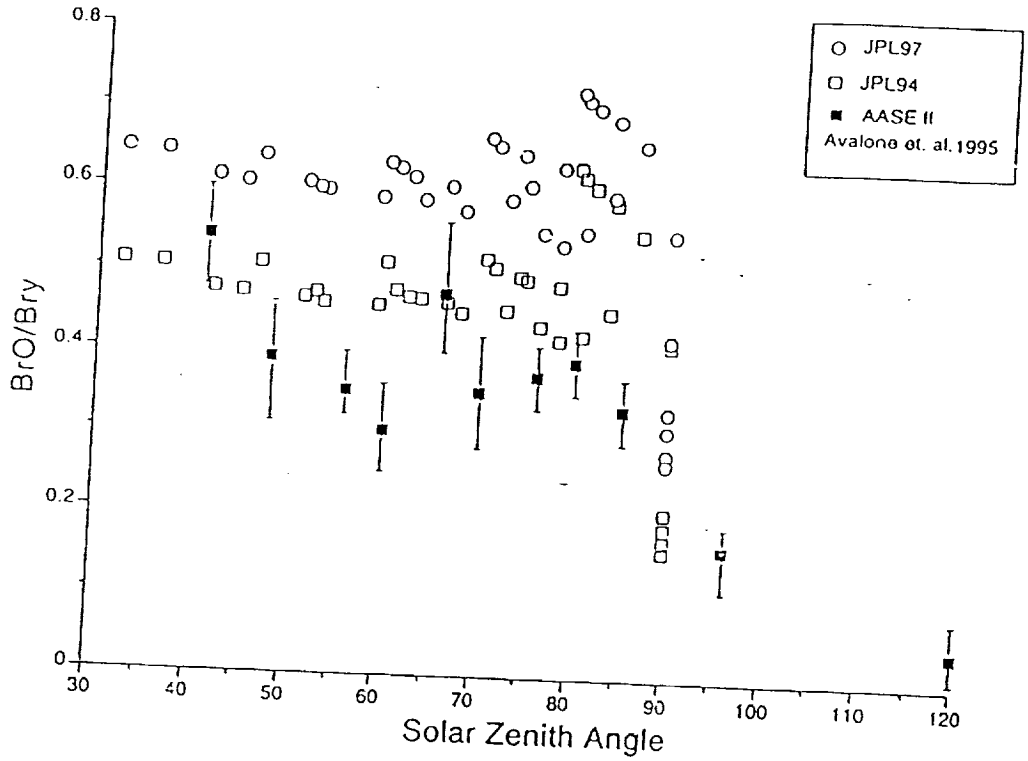

Figure 2b: Same as figure 2a except that the results are sorted by solar zenith angles.

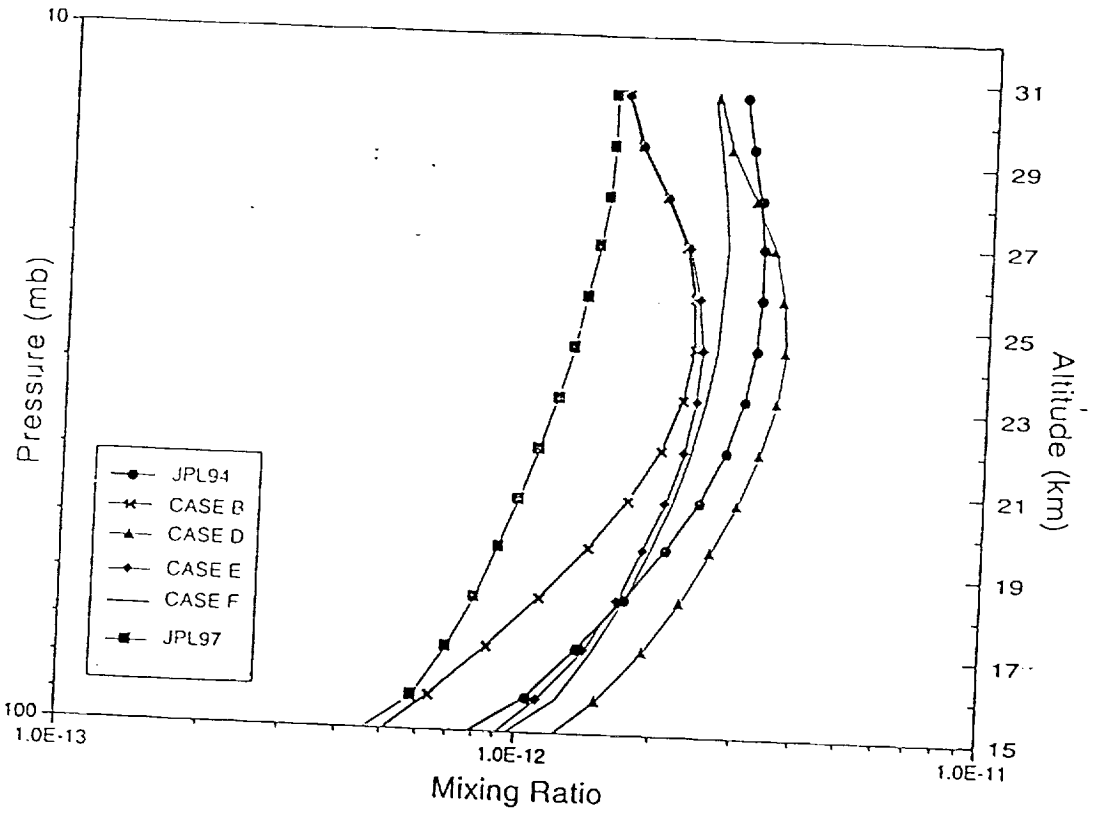

Figure 3: Model calculated day-time average concentration of HOBr for different cases. See Table 3 for the description of the cases.

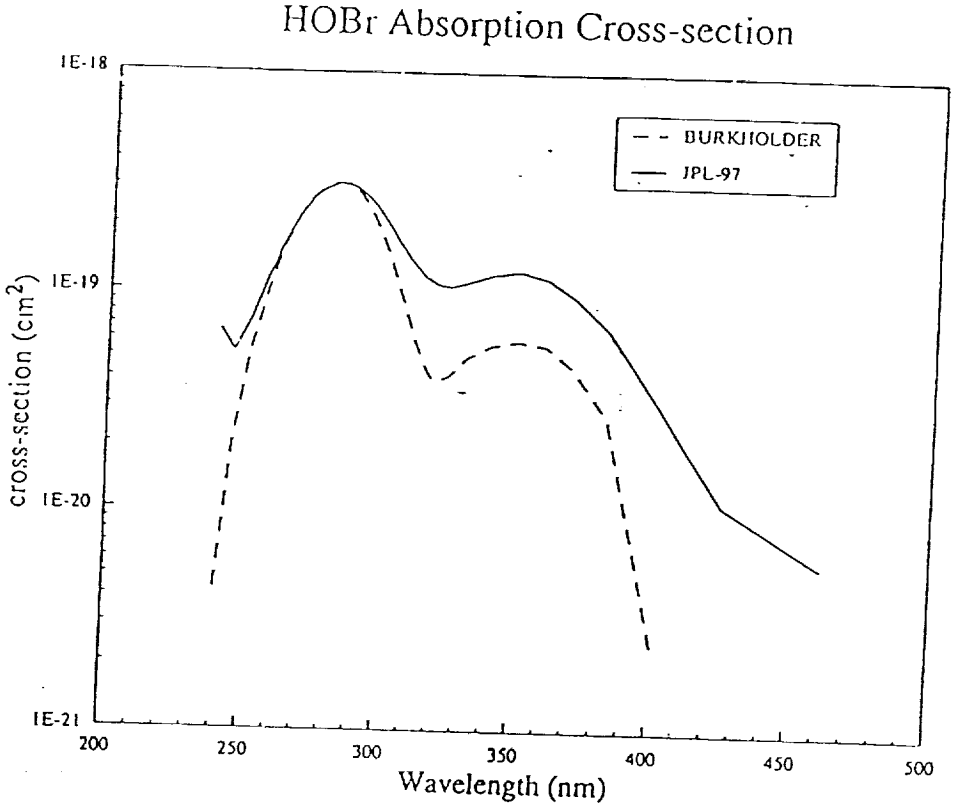

Figure 4: Absorption cross-sections of HOBr from Orlando and Burkholder (1995) and the JPL-97 recommendation.

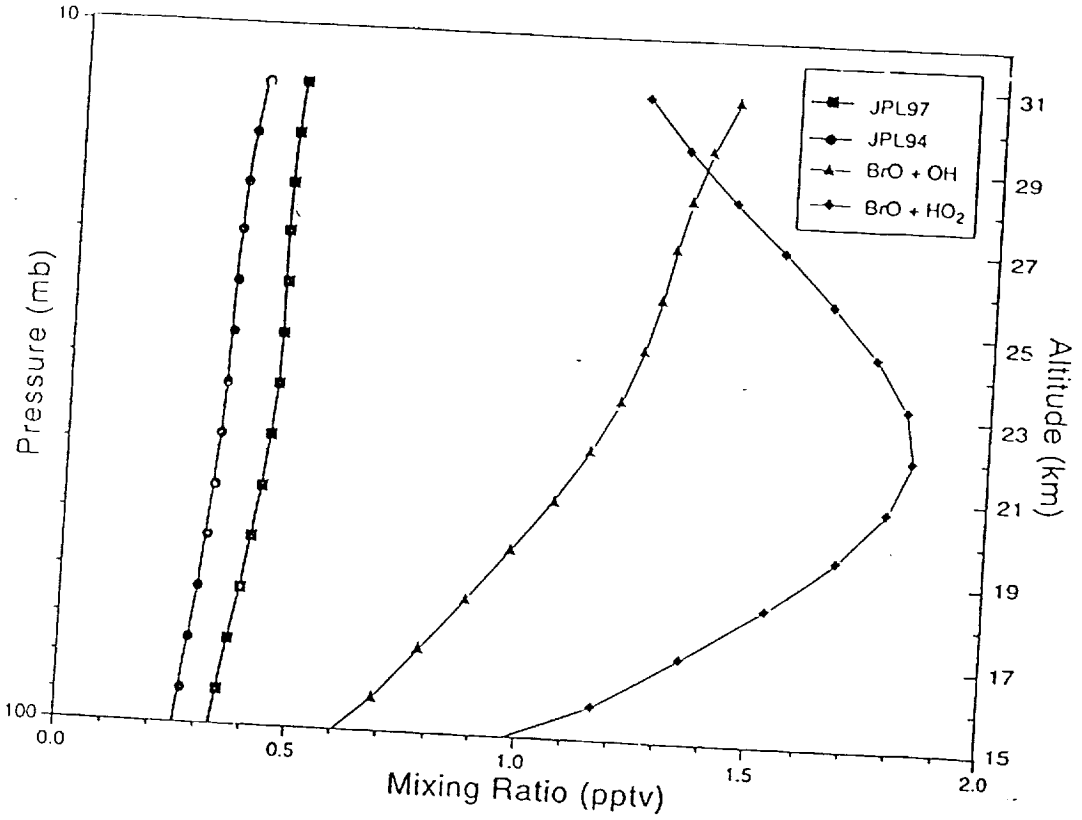

Figure 5: Model calculated mixing ratio profiles for HBr calculated using JPL-94 and JPL-97 rate data recommendations. The curve labeled BrO + OH is calculated assuming an HBr yield of 1.3% from the reaction. The curve labeled BrO + HO2 assumes an HBr yield of 0.6% from the reaction.

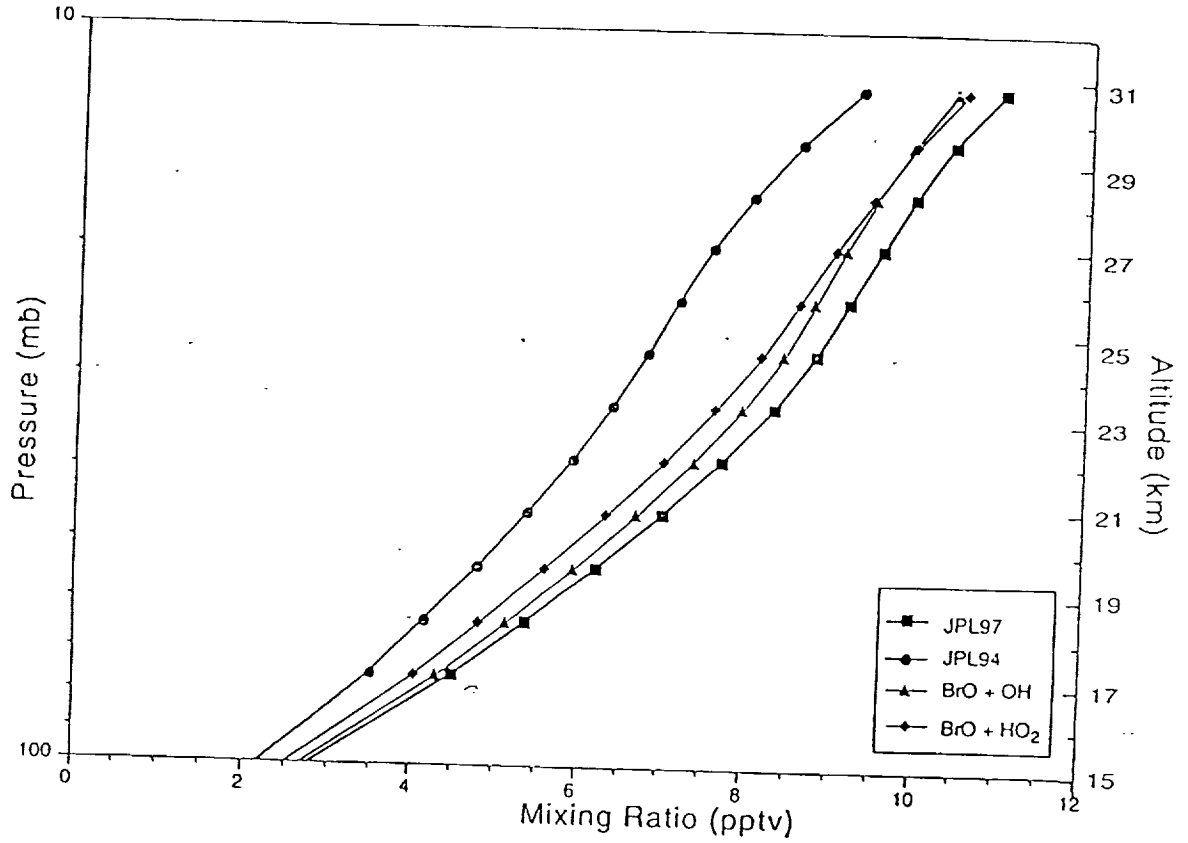

Figure 6: Same as figure 5 except for BrO.

Appendix B

Stratospheric Cooling and Arctic Ozone Recovery

M.Y. Danilin, N.D. Sze, M.K.W. Ko, J.M. Rodriguez

AER, Inc., 840 Memorial Drive, Cambridge, MA 02139, USA

A. Tabazadeh

NASA Ames Research Center, Moffett Field, CA 94035, USA

Abstract

Recent winter/spring observations in the Arctic [Manney et al., 1996,1997; Müller et al., 1997; Rex et al., 1997] reveal further reductions of the ozone content despite near complete disappearance of Pinatubo aerosol from the stratosphere [Thomason et al., 1997] and essentially constant levels of chlorine and bromine loading [WMO, 1995]. Existing photochemical models of the stratosphere with heterogeneous chemistry predict little or no further stratospheric ozone depletion, unless an alternative mechanism is invoked. One such mechanism could be the cooling of the lower stratosphere [Oort and Liu, 1993; Randel and Cobb, 1994; Ramaswamy et al., 1996] leading to triggering of polar stratospheric cloud (PSC) formation. As a result, chlorine activation by enhanced PSCs provides further ozone decline during the winter/spring period. Here, we present sensitivity study results of the AER box model for typical conditions in the lower stratosphere at 70°N during the December 1 - April 1 period for an idealized parcel with different assumed stratospheric coolings and chlorine loadings. Our calculations show that the imposed stratospheric cooling could further deplete ozone and retard its expected recovery even with the projected chlorine loading decrease. We show that, for the present conditions, a 1 K cooling could provide the same local ozone depletion as an increase of chlorine by 0.40-0.95 ppbv for the scenarios considered. Thus, sustained stratospheric cooling could further reduce Arctic ozone content and delay the anticipated ozone recovery in the Northern hemisphere even with the realization of the Montreal Protocol and its Amendments.

Introduction

It is now widely accepted that the spring ozone hole, first detected in Antarctica [Farman et al., 1985; Chubachi et al., 1985], can be explained primarily due to activation of chlorine-containing molecules of anthropogenic origin [Molina and Rowland, 1974] via heterogeneous

reactions on PSC surfaces and their subsequent photolysis [Solomon et al., 1986; McElroy et al., 1986; Molina and Molina, 1987]. The Montreal Protocol with its Amendments are aimed to curb the emissions of chlorofluorocarbons (CFCs), eliminating their production after the year 2000 [WMO, 1995] thus avoiding further depletion of the global ozone layer [Prather et al., 1996]. However, concerns still remain whether an ozone depletion threat can be completely avoided. Recent satellite [Manney et al., 1996,1997; Newman et al., 1997], ozonesondes, and ground-based [Bojkov et al., 1995; Fioletov et al., 1997] measurements clearly show an alarming level of stratospheric ozone depletion (~30-40% below its climatological values at 20 km altitude and less than 250 D.U. in total column (i.e. ~30-40% below climatological values)) in the Northern Hemisphere during last two winters/springs. According to the current understanding, these large values of ozone depletion are surprising, since the Pinatubo aerosol has been mainly removed [Thomason et al., 1997] and the level of chlorine and bromine loading remains almost constant [WMO, 1995]. However, more detailed meteorological analysis reveals low temperatures in the stratosphere [Manney et al., 1997; Fioletov et al., 1997] and a stable longer-lasting polar vortex [Coy et al., 1997] during the past winter.

The purpose of this study is to investigate the ozone behavior within an idealized typical air parcel in the Arctic stratosphere under projected declining chlorine loadings superimposed with various assumed cooling trends. We will also show that the time constant associated with ozone recovery in the colder stratosphere could be significantly prolonged. We are addressing neither the reasons or dynamical aspects of stratospheric cooling nor the contributions of different radiatively-active gases to the stratospheric temperature regime. Also, we are not attempting to predict the ozone content above particular locations for particular dates. Our sensitivity study tries to capture a typical year-to-year pattern of the O_3 behavior in the Arctic winter/spring stratosphere. We focus on evaluating the chemical implications of stratospheric cooling assuming, for the sake of simplicity, the same air parcel trajectory and ignoring ozone radiative [Ramaswamy et al., 1996] and dynamical [Rosenfield et al., 1994] feedbacks. Shindell et al [1998], using the GISS 3-D climate model with sophisticated radiative and dynamical codes but with simplified chemistry, showed that the chemical mechanism plays the dominant role in the polar ozone recovery for the projected chlorine and greenhouse gas loadings, thus making our analysis particularly relevant.

Initialization of the AER Box Model

Photochemical box models have been applied successfully to analyze different aspects of the Antarctic ozone hole [e.g. Schoeberl et al., 1996; Danilin et al., 1996; Kawa et al., 1997]. For this study, we use the AER photochemical box model with the heterogeneous chemistry package described in Danilin et al. [1996]. We investigate chemical effects in the lower stratosphere, since the ozone profile has its maximum there and its perturbation due to PSC processing is also strongest there, thus determining to a large extent the magnitude of total ozone column depletion. So our box model calculations in the lower stratosphere could serve as a proxy of the ozone column change. We simulate the behavior of an isolated air parcel at a latitude of 70°N subsiding with a rate of 1 km/month from ~24 km on December 1 to ~20 km on April 1 [Rosenfield et al., 1994]. The latitude of 70°N for our calculations is chosen because this latitude is *typically* located within the polar vortex according to analysis of zonal fields of potential vorticity [Manney et al., 1994]. We constrain initial concentrations in the air parcel using the UARS data in a fashion similar to Carslaw et al [1997a]. Initial mixing ratios of O_3 (3.6 ppmv), HCl (1.7 ppmv), H_2O (5 ppmv), and CH_4 (1 ppmv) are chosen based on the HALOE measurements on December 1 at our starting point (70°N, 32 hPa). Initial values of $ClONO_2$ (1.2 ppbv) and HNO_3 (11.5 ppbv) are taken from the CLAES measurements [Roche et al., 1994]. We assume 3 ppbv of Cl_y (=Cl + ClO + HCl + $ClONO_2$ + HOCl + 2(Cl_2O_2 + Cl_2)), 14 ppbv of NO_y (= HNO_3 + NO + NO_2 + NO_3 + HNO_4 + HONO + $2N_2O_5$ + $ClONO_2$) and 20 pptv Br_y (= Br + BrO + HOBr + $BrONO_2$ + BrCl + HBr) consistent with the CLAES measurements N_2O using the N_2O-NO_y [Loewenstein et al., 1993], N_2O-Cl_y [Woodbridge et al., 1995], and N_2O-Br_y [R.Salawitch, personal communication] correlations. Initial partitioning among the rest of the chlorine, bromine, and nitrogen species is taken from the AER 2-D model [Weisenstein et al., 1996]. We also assume decrease of NO_y in the air parcel from 14 ppbv on December 1 to 10.2 ppbv in late March to be consistent with MLS HNO_3 measurements [Santee et al., 1997]. Initial aerosol surface area density (SAD) is equal to 1.8 $\mu m^2/cm^3$ with assumed log-normal distribution with mean diameter of 0.155 μm and width σ=1.49, consistent with the aircraft measurements for the background conditions used in Carslaw et al [1994]. The aerosol SAD is kept constant during the NAT runs and is variable during the STS runs due to uptake of HNO_3 and H_2O. The shape of the temperature history chosen in this study (see Figure 1) mimics the evolution of the vortex-averaged minimum temperature in the lower stratosphere

[Zurek et al., 1996] but is increased uniformly by 5 K to provide ~30% ozone depletion at the point of interest during a model run from December 1 to April 1. This temperature shift serves as a 'tuning' parameter. We also do not superimpose 6-10 day waves on our temperature history (like in [Carslaw et al., 1997a]) to avoid additional complications of the day-to-day variability of PSCs, which could mask the main point of our study.

Type I PSC schemes

One of the key uncertainties for our analysis is what PSC scheme should be adopted for the model runs. The issue of how type I PSCs are formed is still a subject for discussion [Carslaw et al., 1994, 1997b; Tabazadeh et al., 1994; Tolbert, 1994]. However, the model analysis by Sessler et al. [1996] shows that, evaluating the chlorine activation and consequent ozone depletion, a whole spectrum of type I PSC formation possibilities is embraced by the nitric acid trihydrade ($HNO_3 \bullet 3H_2O$, NAT) and supercooled ternary solution ($H_2SO_4/HNO_3/H_2O$, STS) schemes. Our box model allows type I PSCs formation via NAT without supersaturation (with fixed diameter of 1 μm) or via STS [Tabazadeh et al., 1994]. The comparative efficacy of chlorine activation in these schemes also depends on the assumed level of background sulfate aerosol and size of NAT particles. Figure 2 addresses differences between these two schemes from the point of view of SAD available for heterogeneous reactions in the NAT and STS schemes as well as the reaction probabilities and e-folding times of the principal chlorine activation reaction $ClONO_2 + HCl \longrightarrow Cl_2 + HNO_3$. A very steep increase of the reaction probability and surface area with decreasing temperature below 196 K drastically reduces the e-folding time of chlorine activation from ~200 hours at 196 K to 1.5-3 hours at 191 K. For the particular parameters of this study, the STS scheme is more efficient below 191 K, while a steep increase of the the NAT SAD between 195 and 192 K makes the NAT scheme slightly more efficient than STS scheme in this temperature range. Figure 2 also shows that it is barely possible to use ClO measurements to distinguish the NAT and STS schemes for the air parcels exposed to low temperatures for a long time (days or so), since all chlorine is expected to be activated in both schemes. Additionally, Figure 2 can demonstrate why the ozone hole has been first observed in the Southern (but not in the Northern hemisphere) in the 1980s. Colder temperature in the Antarctic lower stratosphere (by 7-8 K comparing with the Arctic stratosphere) and more stable polar vortex greatly facilitates chlorine activation, thus producing stronger ozone depletion for the same or

slightly lower level of Cl_y there compared with that in the Arctic.

Equivalence of stratospheric cooling and increase of chlorine loading

To investigate the sensitivity of the ozone depletion to a wide range of chlorine loading and stratospheric cooling, we performed model runs for 2 to 3.5 ppbv Cl_y and 0 to 5 K stratospheric cooling. Effects of stratospheric cooling are investigated by lowering the whole temperature pattern by 1 to 5 K while keeping its shape unchanged as shown in Figure 1. The change of ozone mixing ratio in the air parcel on April 1 as a percentage of its initial value of 3.6 ppmv is plotted as a function of chlorine loading and further stratospheric cooling in Figure 3. This figure summarizes our findings and underlines the widely accepted point that ozone content decreases with increasing level of Cl_y (draw any horizontal line in Figure 3). However, this figure also clearly shows that possible further stratospheric cooling (due to CO_2 or H_2O [IPCC, 1995; WMO, 1995]) has the effect equivalent to an increase of chlorine loading from the ozone balance point of view.

In order to further elucidate results in Figure 3, we introduce "chlorine-cooling equivalent" (CCE) as a measure of the change in chlorine loading equivalent to a 1 K cooling for a given level of the ozone depletion in the air parcel under specified ambient conditions. Our results for the NAT scenario show, for example, that 30% decrease of the ozone mixing ratio in the air parcel could result from either 3.1 ppbv Cl_y and T_{base}, or 2.15 ppbv Cl_y and T_{base}-1K. In other words, a 1 K cooling produces the same effect in the local ozone content as an increase of Cl_y by 0.95 ppbv (i.e. the cooling-chlorine equivalent is equal to $\sim$ 0.95 ppbv(Cl_y)/K). For the STS scenario, the ozone sensitivity to cooling is smaller (CCE$\approx$0.4 ppbv(Cl_y)/K for the 30% depletion isoline). The higher values of the CCE for the NAT runs can be explained by the very steep increase of the NAT SAD for the chosen present day case (see Figures 1 and 2). However, further cooling leads to the saturation of the NAT SAD due to complete conversion of HNO_3 from gas to solid phase, thus lowering the CCE values to several tenth of ppbv(Cl_y)/K. The similar pattern is observed for the STS scenario, thus showing that the CCE concept developed here remains valid for the different PSC schemes. The absolute values of the CCE is a non-trivial function of the chosen ozone depletion, ambient atmospheric conditions, and chosen PSC scheme. The CCE is a local parameter and should not be extrapolated to the global scale. However, the concept of CCE, applied in more sophisticated global models, could be useful in regulatory discussions. One can

also introduce a carbon dioxide - chlorine loading equivalent or ozone depletion potential (ODP) of CO_2 which could help to formulate a future regulatory ozone protection policy translating CO_2 emissions to CFCs emissions after proper scaling using global model calculations. The WMO [1995] Report does not consider CO_2 as an ozone depleting species.

Our calculations for Antarctic conditions (similar to [Danilin et al., 1996] and not shown here) show CCE values $\approx$0.15 ppbv(Cl_y)/K there. This implies that possible future cooling of the Antarctic stratosphere would have a smaller effect on ozone depletion (which is close already to its saturation level [Hofmann et al., 1997]) than similar cooling in the Arctic.

Discussion and outlook

As a continuation of our sensitivity analysis, we present calculations of ozone behavior along the idealized air parcel considered in the previous sections using anticipated future level of chlorine loading and assumed stratospheric cooling. We follow the WMO scenarios for the Cl_y (shown by solid black line in Figure 4) and CH_4 concentrations assuming a fixed level of Br_y (=20 pptv). Figure 4 shows that, ignoring stratospheric cooling, one indeed should anticipate a steady recovery of ozone (green lines) in the lower stratosphere immediately after reduction of the Cl_y loading peaking at the level of 3.08 ppbv at 24 km (or $\sim$3.7 ppbv at the top of the stratosphere) in the year 2000. The red dashed line shows "the road not taken" [Prather et al., 1996], assuming the level of chlorine is fixed at 3 ppbv and stratospheric cooling with a rate of -0.15 K/year. However, even for the relatively modest constant temperature trend of -0.05 K/year [Randel et al., 1994; Ramaswamy et al., 1995], ozone remains below its 1995-level for the next fifty years in the NAT scenario. For the STS scenario, ozone returns to the 1995-content near the year 2030. For the larger temperature trend of -0.1 K/year, further delay of the ozone recovery is expected with more than 40% ozone depletion, keeping the ozone content in the parcel below its 1995 level during next 50 years in the both scenarios. For the more severe cooling rate of -0.15 K/year, a larger ozone depletion is calculated (more than -40%) with a longer-lasting impact. For the considered scenarios, the maximum ozone depletion could be anticipated during the 2010-2020 period for all temperature trends and both PSC scenarios. Thus, our calculations show that the ozone depletion in the Arctic stratosphere may be deepened and its recovery delayed by several decades when stratospheric cooling is taken into account. Both our results and the 3-D climate model calculations of Shindell et al [1998] show

that the currently accepted anticipation of ozone healing in the Arctic following the elimination of CFCs emissions may be too optimistic.

Our results show that the Arctic ozone is very sensitive to the ambient temperature in the lower stratosphere. We present estimates of only the chemical effects of stratospheric cooling. Stolarski [1997] discussed three possible scenarios of future development of the Arctic ozone, depending on what the main reason of the observed stratospheric cooling is: a) greenhouse gases, b) ozone, or c) just natural variability. Since the natural variability of the Arctic winter stratosphere is large and relevant data sets are short, it is difficult to determine the cause of the observed cooling. Each cause could have important implications. a) Carbon dioxide provides the strongest cooling in the lower stratosphere among greenhouse gases (e.g. IPCC [1995], Clough and Iacono [1995]). If the cooling and the polar ozone hole propagate upwards in the near future, it could be considered a manifestation of greenhouse gas effects due to the vertical profiles of the CO_2 cooling rate [e.g. Clough and Iacono, 1995]. In this case, the extent of polar stratospheric ozone depletion could become considerably larger and its recovery delayed by several decades even with the implementation of the Montreal Protocol. If future polar measurements and more sophisticated 3-D calculations support our findings, CO_2 emissions should be contained for better ozone protection.

b) Ozone itself is a very important radiative species and there is a strong coupling between radiative, chemical, and dynamical processes in the Arctic stratosphere. In this case, more sophisticated 3-D model calculations with all these feedbacks and a state-of-the-art stratospheric heterogeneous chemistry module [e.g. Austin et al., 1992] are required to predict future cooling and evolution of the possible Arctic ozone hole.

c) It is also possible that current stratospheric conditions represent a complicated mixture of natural variability and human impact. If this is true, further model prediction of the Arctic stratospheric ozone recovery is an extremely complex issue.

Since the current atmospheric conditions in the Arctic are very close to conditions allowing further steep ozone loss via an additional PSC formation, a very careful analysis of the consequences of current or future levels of emissions, which directly (e.g. aircraft H_2O and NO_x) or indirectly (CO_2) facilitate the formation of PSCs or provide additional sites (aircraft sulfate particles) for heterogeneous chlorine activation, is required [Peter et al., 1991; Weisenstein et al., 1996; DelNegro et al., 1997]. Our previous study shows a possibility that severely depleted

ozone in the polar region could be diluted to the mid-latitudes after the final stratospheric warming [Sze et al., 1989]. A more detailed study of the reasons for the lower stratospheric cooling with particular emphasis on anthropogenic contributions to this effect and consequent effects on ozone at polar and middle latitudes will require a use of a 3-D model with all necessary feedbacks.

Acknowledgments. The work at AER was sponsored by NASA Atmospheric Chemistry Modeling and Analysis (NAS5-97039) and UARS Guest Investigator Programs (NAS5-32844). We thank M.L. Santee, G.L. Manney, P.A. Newman, L. Coy, V.E. Fioletov, and D.T. Shindell for relevant discussions and sending their unpublished manuscripts.

References

Austin, J., N. Butchart, and K.P. Shine, Possibility of an Arctic ozone hole in a doubled-CO_2 climate, *Nature, 360,* 221-225, 1992.

Bojkov, R.D., L. Bishop, and V.E. Fioletov, Total ozone trends from quality controlled ground-based data (1964-1994), *J. Geophys. Res., 100,* 25,867-25,876, 1995.

Carslaw, K.S. et al., Stratospheric aerosol growth and HNO_3 gas phase depletion from coupled HNO_3 and water uptake by liquid particles, *Geophys. Res. Lett., 21,* 2479-2482, 1994.

Carslaw, K.S., T. Peter, and R. Müller, Uncertainties in reactive uptake coefficients for solid stratospheric particles: 2.Effect on ozone depletion, *Geophys. Res. Lett., 24,* 1747-1750, 1997a.

Carslaw, K.S., T. Peter, and S.L. Clegg, Modeling the composition of liquid stratospheric aerosols, *Rev. Geophys., 35,* 125-154, 1997b.

Chubachi, S., A special ozone observation at Syowa Station (Antarctica) from February 1982 to January 1983, In: Atmosph. Ozone (eds. C.S. Zerefos and A.M. Ghazi), 285-289, 1985.

Clough, S.A., and M.J. Iacono, Lyne-by-line calculation of atmospheric fluxes and cooling rates: 2. Application to carbon dioxide, ozone, methane, nitrous oxide and the halocarbons, *J. Geophys. Res., 100,* 16,519-16,535, 1995.

Coy, L., P.A. Newman, and E.R. Nash, Meteorology of the polar vortex: Spring 1997, *Geophys. Res. Lett., 24,* 2693-2696, 1997.

Danilin, M.Y., N.D. Sze, M.K.W. Ko, J.M. Rodriguez, and M.J. Prather, Bromine-chlorine coupling in the Antarctic ozone hole, *Geophys. Res. Lett, 23,* 153-156, 1996.

DelNegro, L.A., et al., Evaluating the role of NAT, NAD, and liquid $H_2SO_4/H_2O/HNO_3$ solutions in Antarctic PSC aerosol: Observations and implications, *J. Geophys. Res., 102,* 13,255-13,282, 1997.

Farman, J.C., B.G. Gardiner, and J.D. Shanklin, Large losses of total ozone in Antarctica reveal seasonal ClO_x/NO_x interaction, *Nature, 315,* 207-210, 1985.

Fioletov, V.E., et al., Long-term decline of ozone over the Canadian Arctic until early 1997 from ground-based and balloon sonde measurements, *Geophys. Res. Lett., 24,* 2705-2708, 1997.

Hanson, D.R., and A.R. Ravishankara, Reaction of $ClONO_2$ with HCl on NAT, NAD and frozen sulfuric acid and hydrolysis of N_2O_5 and $ClONO_2$ on frozen sulfuric acid, *J. Geophys. Res., 98,* 22,931-22,936, 1993.

Hanson, D.R., and A.R. Ravishankara, Reactive uptake of $ClONO_2$ onto sulfuric acid due to reaction with HCl and H_2O, *J. Phys. Chem., 98,* 5728-5735, 1994.

Hofmann, D.J., et al., Ten years of ozonesonde measurements at the south pole: Implications for recovery of springtime Antarctic ozone, *J. Geophys. Res., 102,* 8931-8943, 1997.

IPCC Climate Change, *Cambridge Univ. Press,* Cambridge, 572 pp., 1995.

Kawa, R.S., et al., Activation of chlorine in sulfate aerosol as inferred from aircraft observations, *J. Geophys. Res., 102,* 3921-3934, 1997.

Loewenstein, M., et al., New observations of the NO_y-N_2O correlation in the lower stratosphere, *Geophys. Res. Lett., 20,* 2531-2534, 1993.

Manney, G.L. et al., The anomalous Arctic lower stratospheric polar vortex of 1992-1993, *Geophys. Res. Lett., 21,* 2405-2408, 1994.

Manney, G.L., M.L. Santee, L. Froidevaux, J.W. Waters, and R.W. Zurek, Polar vortex conditions during the 1995-96 Arctic winter: Meteorology and MLS ozone, *Geophys. Res. Lett., 23,* 3203-3206, 1996.

Manney, G.L., L. Froidevaux, M.L. Santee, R.W. Zurek, and J.W. Waters, MLS observations of Arctic ozone loss in 1996-97, *Geophys. Res. Lett., 24,* 2697-2700, 1997.

McElroy, M.B., R.S. Salawitch, S.C. Wofsy, and J.A. Logan, Reductions of Antarctic ozone due to synergistic interactions of chlorine and bromine, *Nature, 321,* 759-762, 1986.

Molina, M.J. and F.S. Rowland, *Nature, 249,* 810-814, 1974.

Molina, L.T., and M.J. Molina, Production of Cl_2O_2 from the self-reaction of the ClO radical, *J. Phys. Chem., 91,* 433-436, 1987.

Müller, R. et al., Severe chemical ozone loss in the Arctic during the winter of 1995-96, *Nature, 389*, 709-712, 1997.

Newman, P.A., J.F. Gleason, R.D. McPeters, and R.S. Stolarski, Anomalously low ozone over the Arctic, *Geophys. Res. Lett., 24*, 2689-2692, 1997.

Oort, A.H., and H. Liu, Upper-air temperature trends over the globe, *J. Climate, 6,* 292-307, 1993.

Peter, T., C. Brühl, and P.J. Crutzen, Increase in the PSC-formation probability caused by high-flying aircraft, *Geophys. Res. Lett., 18*, 1465-1468, 1991.

Prather, M.J. et al., The ozone layer: the road not taken, *Nature, 381,* 551-554, 1996.

Ramaswamy, V., M.D. Schwartzkopf, and W.J. Randel, Fingerprint of ozone depletion in the spatial and temporal pattern of recent lower-stratospheric cooling, *Nature, 382,* 616-618, 1996.

Randel, W.J. and J.B. Cobb, Coherent variations of monthly mean total ozone and lower stratospheric temperature, *J. Geophys. Res., 99,* 5433-5447, 1994.

Rex, M., et al., Prolonged stratospheric ozone loss in the 1995-96 Arctic winter, *Nature, 389*, 835-838, 1997.

Roche, A.E. et al., Observations of lower-stratospheric $ClONO_2$, HNO_3, and aerosol by the UARS CLAES experiment between January 1992 and April 1993, *J. Atm. Sci., 51*, 2877-2902, 1994.

Rosenfield, J.E., P.A. Newman, and M.R. Schoeberl, Computations of diabatic descent in the stratospheric polar vortex, *J. Geophys. Res., 99*, 16,677-16,689, 1994.

Santee, M.L., et al., MLS observations of ClO and HNO_3 in the 1996-97 Arctic polar vortex, *Geophys. Res. Lett., 24*, 2713-2716, 1997.

Schoeberl, M.R., et al., Development of the Antarctic ozone hole, *J. Geophys. Res., 101*, 20,909-20,924, 1996.

Sessler, J., et al., What role do type I PSC and aerosol parameterizations play in modelled lower stratosphere chlorine activation and ozone loss? *J. Geophys. Res., 101*, 28817-28835, 1996.

Shindell, D.W., D. Rind, and P. Lonergan, The ozone hole may be deepened and recovery delayed by increasing greenhouse gases, *Nature, submitted*, 1998.

Solomon, S., R.R. Garcia, F.S. Rowland, and D.J. Wuebbles, On the depletion of Antarctic

ozone, *Nature, 321*, 755-758, 1986.

Stolarski, R.S., A bad winter for Arctic ozone, *Nature, 389*, 788-789, 1997.

Sze, N.D., et al., Antarctic ozone hole: Possible implications for ozone trends in the southern hemisphere, *J. Geophys. Res., 94*, 11,521-11,528, 1989.

Tabazadeh, A., R.P. Turco, and M.Z. Jacobson, A model for studying the composition and chemical effects of stratospheric aerosol, *J. Geophys. Res., 99*, 12897-12914, 1994.

Thomason, L.W., L.R. Poole, and T. Deshler, A global climatology of stratospheric aerosol surface area density deduced from SAGE II measurements: 1984-1994, *J. Geophys. Res., 102*, 8967-8976, 1997.

Tolbert, M.A., Sulfate aerosol and PSC formation, *Science, 264,* 527-528, 1994.

Weisenstein, D.K., M.K.W. Ko, N.D. Sze, and J.M. Rodriguez, Potential impact of SO_2 emissions from stratospheric aircraft on ozone, *Geophys. Res. Lett., 23,* 161-164, 1996.

WMO Scientific Assessment of Ozone Depletion: 1994, Rep. 37, Geneva, 1995.

Woodbridge, E.L. et al., Estimates of total organic and inorganic chlorine in the lower stratosphere from in situ and flask measurements during AASE II, *J. Geophys. Res., 100*, 3057-3064, 1995.

Zurek, R.W., et al., Interannual variability of the north polar vortex in the lower stratosphere during the UARS mission, *Geophys. Res. Lett., 23*, 289-292, 1996.

Figure captions

Figure 1. The temperature history adopted for the box model runs at 70°N: solid black line show the present day case; black dashed lines depict the present day case lowered by 1, 2, 3, 4, and 5 K; the almost horizontal dashed lines correspond to the NAT formation threshold and the ice frost point, respectively (their slope is due to a subsidence with the fixed H_2O mixing ratio of 5 ppmv).

Figure 2. Top panel: Calculated surface area density of STS (solid red line) and NAT (solid blue line) particles in $\mu m^2/cm^3$ (left vertical axis) and reaction probability (right vertical axis) of the $ClONO_2 + HCl \longrightarrow Cl_2 + HNO_3$ reaction on STS [Hanson and Ravishankara, 1994] (dashed red line) and NAT [Hanson and Ravishankara, 1993] (dashed blue line) as a function of temperature. Surface area of NAT was calculated assuming its unimodal distribution with

diameter of 1 μm and density 1.62 g/cm^3. Below 205 K, the model of Tabazadeh et al [1994] is used to calculate swelling of aerosol particles due to additional uptake of H_2O and HNO_3. Bottom panel: Timescale of the $ClONO_2 + HCl \longrightarrow Cl_2 + HNO_3$ reaction (defined as $\tau = 4/(\gamma \times \text{SurfaceArea} \times \text{Speed}_{ClONO2}$, in hours) on the STS (red) and NAT (blue) shows an effectiveness of chlorine activation as a function of temperature. Black symbols show minimum temperature during the model runs from 195.25 K (present day case) to 190.25 K (present day case-5K).

Figure 3. Isolines of ozone change in the air parcel on April 1 (in % from its initial value of 3.6 ppmv) as a function of chlorine loading and stratospheric cooling at 20 km and 70°N for the NAT (top panel) and STS (bottom panel) scenarios. These values correspond to constant Br_y=20 pptv and the temperature evolution shown in Figure 1 (i.e. zero cooling correspond to the T_{base} line and 5K cooling - to the T_{base}-5K line shown in Fig.1).

Figure 4. Ozone depletion as function of year for the projected chlorine and methane loading and different rate of stratospheric cooling for the NAT (top panel) and STS (bottom panel) scenarios. Bromine loading is assumed to be constant at 20 pptv. The black line in the bottom panel shows the adopted decrease of chlorine loading at the starting point of the air parcel at 32 hPa. We considered scenarios when the present temperature pattern (Fig.1) remains constant (green curves) and uniformly lowered at a rate of 0.05 K/year (blue curves), 0.1 K/year (cyan curves), and 0.15 K/year (red curves). Ozone change in the parcel for the constant level of chlorine loading at 3 ppbv for the adopted cooling rate of 0.15 K/year is shown by the pink dashed lines.

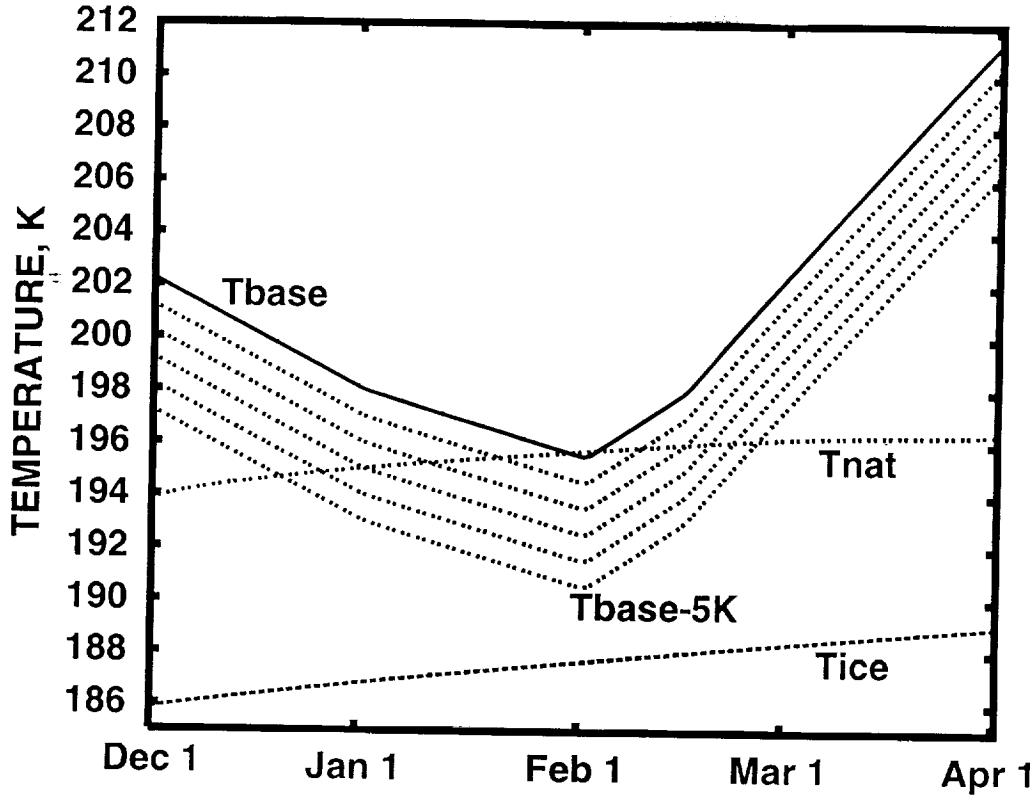
212
210
208
206
204
202
200
198
196
194
192
190
188
186
TEMPERATURE, K
Tbase
Tnat
Tbase-5K
Tice
Dec 1
Jan 1
Feb 1
Mar 1
Apr 1

FIGURE 1

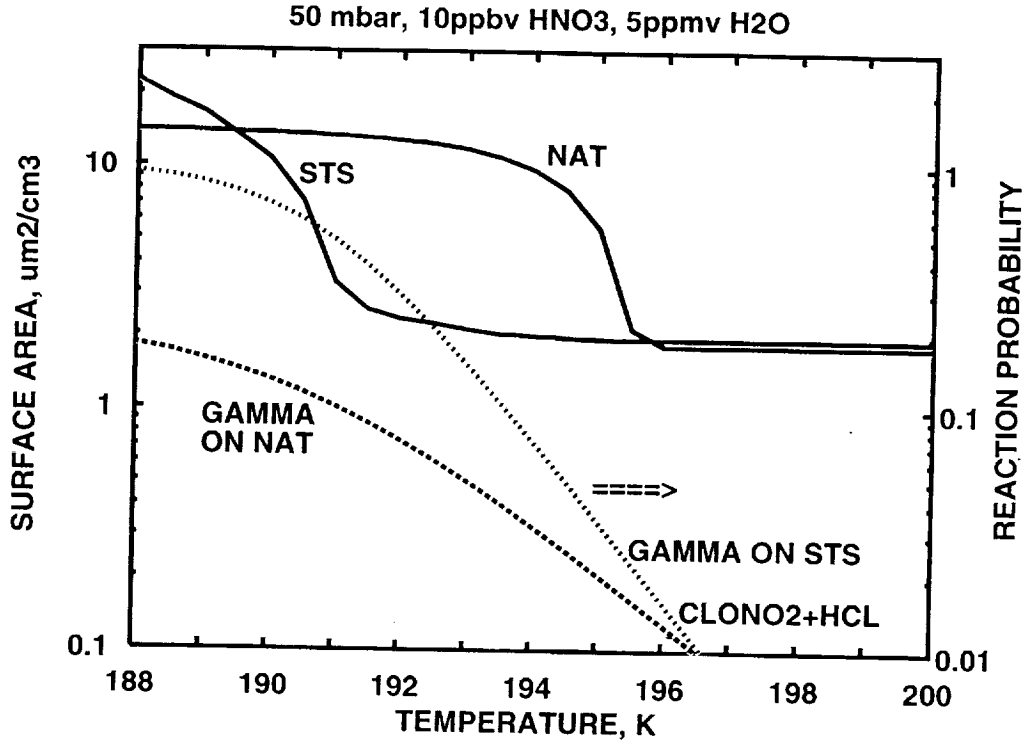
50 mbar, 10ppbv HNO3, 5ppmv H2O
SURFACE AREA, um2/cm3
REACTION PROBABILITY
10
1
0.1
1
0.1
0.01
NAT
STS
GAMMA
ON NAT
====>
GAMMA ON STS
CLONO2+HCL
188
190
192
194
196
198
200
TEMPERATURE, K

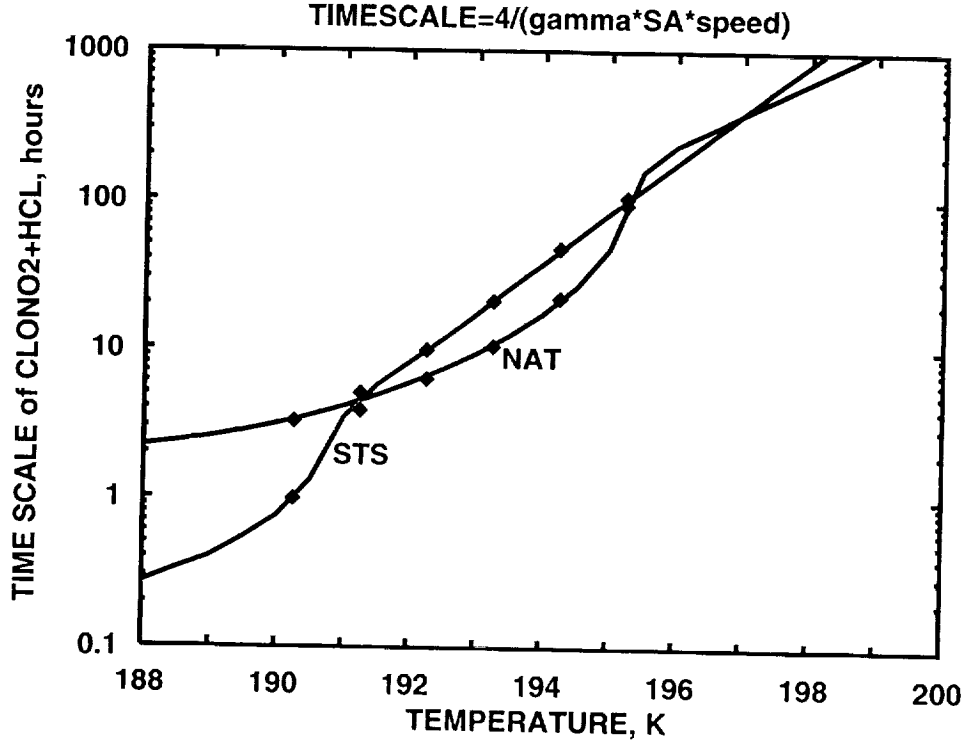
TIMESCALE=4/(gamma*SA*speed)
TIME SCALE of CLONO2+HCL, hours
1000
100
10
1
0.1
NAT
STS
188
190
192
194
196
198
200
TEMPERATURE, K

FIGURE 2.

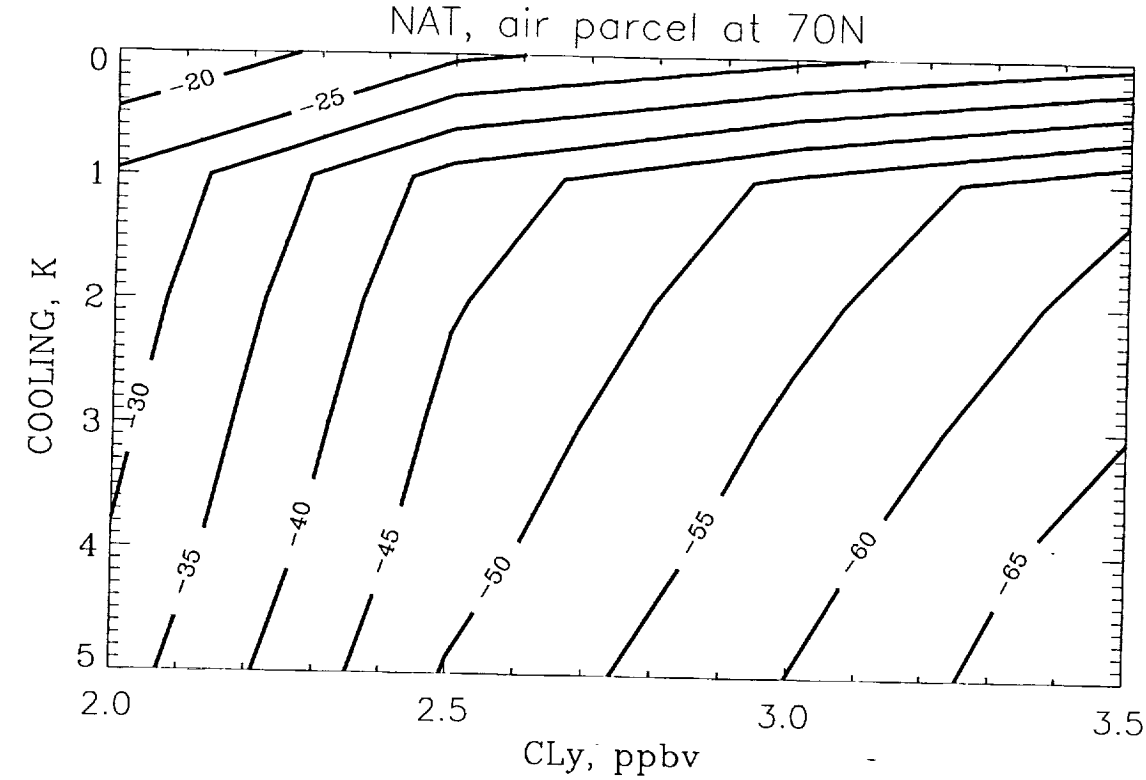
NAT, air parcel at 70N
COOLING, K
CLy, ppbv
0
1
2
3
4
5
2.0
2.5
3.0
3.5
-20
-25
-30
-35
-40
-45
-50
-55
-60
-65

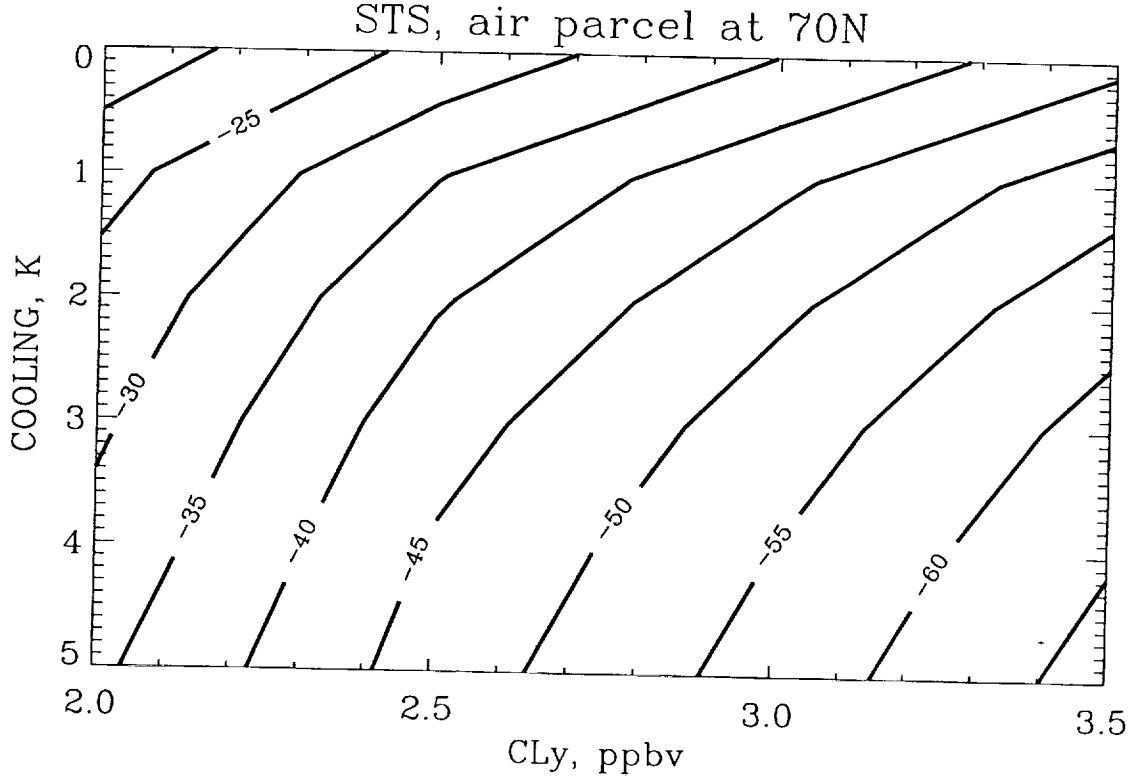
STS, air parcel at 70N
COOLING, K
CLy, ppbv
0
1
2
3
4
5
2.0
2.5
3.0
3.5
-25
-30
-35
-40
-45
-50
-55
-60

Figure 3.

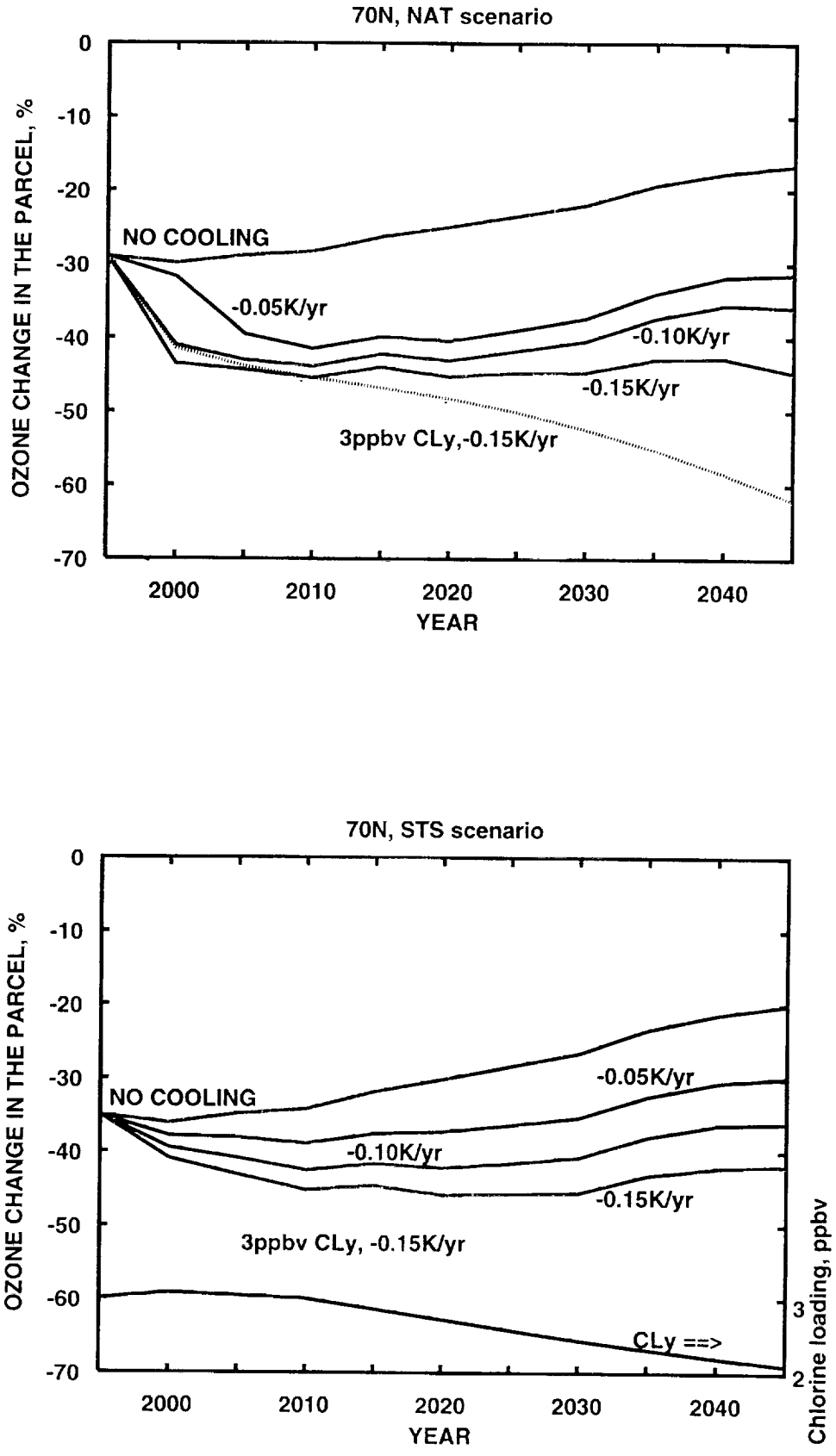
70N, NAT scenario
OZONE CHANGE IN THE PARCEL, %
0
-10
-20
-30
-40
-50
-60
-70
NO COOLING
-0.05K/yr
-0.10K/yr
-0.15K/yr
3ppbv CLy,-0.15K/yr
2000
2010
2020
2030
2040
YEAR
70N, STS scenario
OZONE CHANGE IN THE PARCEL, %
NO COOLING
-0.05K/yr
-0.10K/yr
-0.15K/yr
3ppbv CLy, -0.15K/yr
CLy ==>
Chlorine loading, ppbv
3
2

FIGURE 4.